THE ROLE OF SURFACE PRETREATMENT AND SURFACE ANALYSIS IN THE BONDABILITY OF CARBON FIBER-POLYIMIDE MATRIX COMPOSITES

by

Denise Joy DeGeorge Moyer

Dissertation submitted to the Faculty of the
Virginia Polytechnic Institute and State University
in partial fulfillment of the requirements for the degree of:

DOCTOR OF PHILOSOPHY

in

Chemistry

APPROVED:

J.P. Wightman, Chairman

D.A. Dillard

B.E. Hanson

J.G. Mason

L.T. Taylor

November, 1989

Blacksburg, Virginia

THE ROLE OF SURFACE PRETREATMENT AND SURFACE ANALYSIS IN THE BONDABILITY OF CARBON FIBER-POLYIMIDE MATRIX COMPOSITES

by

Denise Joy DeGeorge Moyer

Committee Chairman: James P. Wightman

Chemistry

(ABSTRACT)

The effect of surface pretreatment on the physical and chemical properties of carbon fiber-polyimide matrix composite surfaces was evaluated. Eight pretreatments were studied: methanol wash, gritblast, sulfuric acid soak, ammonia plasma, argon plasma, argon plasma followed by ammonia plasma, nitrogen plasma, and oxygen plasma. The pretreated surfaces were chemically characterized through the use of XPS (X-ray photoelectron spectroscopy), ISS (ion scattering spectroscopy), and PAS-FTIR (photoacoustic Fourier transform infrared spectroscopy). Surface fluorocarbon contamination was appreciably reduced with gritblasting, argon plasma and oxygen plasma pretreatments. Specific functional groups were incorporated into the composite surfaces through the choice of gases used in the pretreatment. Physical changes were determined through the use of HR-SEM (high resolution scanning electron microscopy). With the exception of the macroroughening produced by gritblasting and the pitting

produced by long exposure times in the oxygen plasma, no significant differences in the topography of the pretreated composites were observed. The wettability of the pretreated composite surfaces increased, as demonstrated with contact angle measurements, due to a combination of a decrease in the fluorocarbon contamination and an increase in the surface functionality present.

LaRC-TPI was used for all priming and adhesive bonding of the pretreated composites. Both the single lap shear test and the wedge test were used to evaluate the effect of surface pretreatment on the strength and durability of the adhesively bonded composite joints. Both types of joints were placed in three different environments: (i) room temperature, desiccator, 1000 hours (ii) 204^{o}C, 1000 hours and (iii) immersion in boiling water, 3 days for single lap shear test, until failure for wedge test. The oxygen plasma was found to be the best pretreatment. The improvement in adhesive bonding following exposure to an oxygen plasma in comparison to all of the other surface pretreatments was attributed to several factors - a reduction in fluorocarbon contamination and an increase in oxygen surface functionality. This increased surface functionality and decrease in fluorocarbon contamination cause better wetting of the composite surface and may also lead to covalent bonding at the composite-primer interface.

Acknowledgements

My sincerest thanks go to my advisor Dr. James P. Wightman for his enthusiasm, scientific guidance and support, and for giving me the opportunity to attend numerous meetings and to meet many fellow scientists.

I would like to extend thanks to my committee members Dr. D.A. Dillard, Dr. B.E. Hanson, Dr. J.G. Mason and Dr. L.T. Taylor for serving on my committee and for helpful technical discussions and suggestions.

I would also like to extend my sincere appreciation to Mr. D.J. Progar and Dr. T.L. St. Clair from the NASA-Langley Research Center for provision of the composite panels and adhesive, for allowing me the opportunity to spend a week at the NASA-LaRC and for helpful technical discussions. I also wish to thank the NASA-LaRC Graduate Student Researchers Program for financial support of this dissertation.

I also extend thanks to and for help in obtaining the HR-SEM photomicrographs, to for his help with the statistical analysis, to for typing of this manuscript, and to my fellow graduate students for their support and helpful discussions. A special thanks to for all of his help, willingness, and patience and for the work he puts into the surface analysis lab.

I must also thank the V.P.I. & S.U. Center for Adhesive and Sealant Science for encouraging an interdisciplinary approach to graduate studies in the area of adhesion.

Finally, I would like to thank my husband, , for many helpful technical discussions and computer assistance; and my parents, , my brother, , my sister, , and my husband, , for their unending support, inspiration, encouragement, patience, understanding and love throughout graduate school.

To my husband, , and my parents.

For the message of the cross is foolishness to those who are perishing, but to us who are being saved it is the power of God. For it is written: "I will destroy the wisdom of the wise; the intelligence of the intelligent I will frustrate." Where is the wise man? Where is the scholar? Where is the philosopher of this age? Has not God made foolish the wisdom of the world?

But God chose the foolish things of the world to shame the wise; God chose the weak things of the world to shame the strong. He chose the lowly things of this world and the despised things - and the things that are not - to nullify the things that are, so that no one may boast before him. It is because of him that you are in Christ Jesus, who has become for us wisdom from God - that is our righteousness, holiness and redemption. Therefore, as it is written: "Let him who boasts boast in the Lord."

I Corinthians 1:18-20, 27-31

TABLE OF CONTENTS

LIST OF TABLES

LIST OF FIGURES

I: INTRODUCTION

Composite materials are continuing to become increasingly important in the fields of materials and structures. Composites are finding increased use specifically in aircraft and spacecraft structures. The rapid growth in the use of composites, specifically as engineering materials, has been achieved because composite materials offer many advantages over traditional materials, such as metals. The features which make composites so promising as engineering materials are their high specific strength (relative strength-to-weight ratio), high specific stiffness (relative stiffness-to-weight ratio) and the opportunity to tailor material properties through the control of fiber and matrix composition and fiber orientation. Also due to a reduction in mass, cost and the total number of components needed, the use of composite materials is advantageous over the use of metallic structures. A weight savings of 10-50 percent is usually achieved with the use of advanced composite materials instead of metallic structures designed to perform the same function (1). Composites are also corrosion resistant and they have a high fatigue resistance.

Although metallic structures may be joined together by a number of methods such as riveting, bolting, welding, bonding, brazing and soldering, only adhesive bonding and mechanical fasteners (bolting and riveting) can be utilized

to join composite materials. Adhesive bonding of composite structures is the preferred technique for numerous reasons. Adhesive bonding provides higher joint efficiency indexes (relative strength-to-weight of the joint region) and an improved stress distribution over mechanical fastening. In drilling the holes, for bolts or rivets, fibers are cut in the composite material weakening the structure to be joined. Also because mechanical fasteners join the structure at discrete points large stress concentrations occur around each hole drilled. Also, mechanical fasteners can be structurally inefficient due to the low shear strengths of composite materials. Superior fatigue resistance, damping characteristics and noise reduction and excellent electrical and thermal insulation are also advantages of using adhesive bonds to join composite materials rather than mechanical fasteners.

Even though adhesive bonding is the preferred technique to join composite materials an increased understanding of composite-adhesive bonding must be obtained so that the full potential of composite materials may be realized. Understanding composite-adhesive bonding involves understanding the interfacial region or "interphase" which is widely accepted as an area that strongly influences the mechanical performance of adhesively bonded composite materials (2). A schematic of the interphase region is shown in Figure 1.1. The interphase considers the interactions

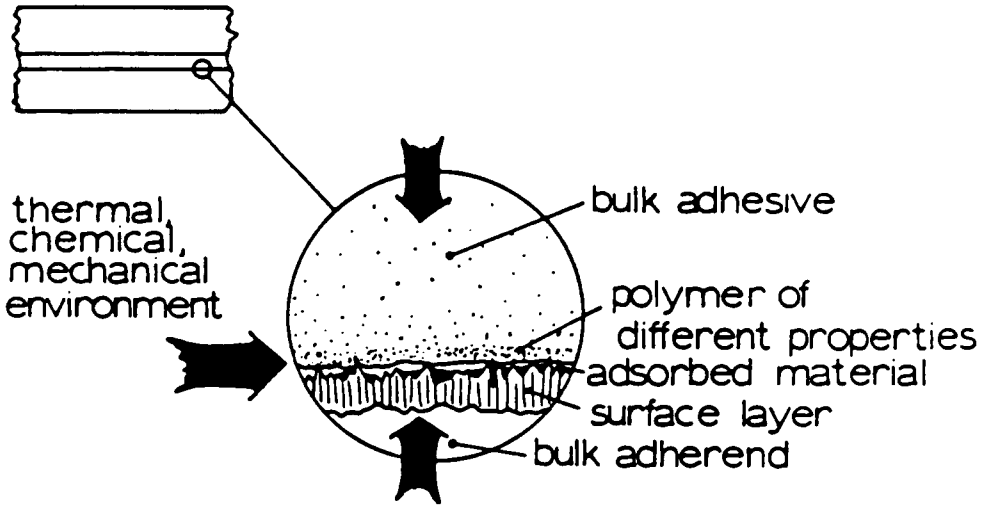

Figure 1.1. Schematic representation of the adhesive-adherend interphase (3).

between the adhesive and the adherend to be three-dimensional rather than two-dimensional. Also the interphase represents an area between the bulk adhesive and the bulk adherend, where the local properties begin to change from the bulk properties of the adherend to the bulk properties of the adhesive, while going through the interface.

The objective of this study was three-fold. The first objective was to better understand the factors which affect the adhesive bonding of composite materials so that the full potential of composite structures may be obtained. Here, the physical and chemical properties of composite surfaces before and after various surface pretreatments were studied. Next, the effect of surface pretreatment on the strength and durability of adhesively bonded composite joints was evaluated. The second objective was to better understand composite-adhesive bonding, in general, in order to evaluate new high temperature adhesives. The final objective was to use the combined results obtained to address the basic question of the role which the interfacial region or the interphase has in determining the performance of adhesively bonded composite joints.

II: LITERATURE REVIEW

This chapter will endeavor to provide some perspective for the original work in the area of surface pretreatment and adhesive bonding of composite materials which will be presented in the chapters to follow. First, a background in the areas of composite materials and high temperature structural polymers and adhesives will be addressed. Then a general review of adhesive bonding, including theories of adhesion, bonding configurations and surface pretreatments will be presented. The literature dealing with any individual aspect of this work is quite extensive, therefore only the area of the effect of surface pretreatment on composite-composite bonding will be thoroughly reviewed.

A. Composite Materials

There is no universally accepted definition of composite materials. Definitions in the literature differ widely and many materials can be classified as composites. In the dictionary, the term "composite" refers to something made up of distinct parts. Of all composite materials, the fiber type, specifically the inclusion of fibers in a matrix, has generated the most interest among engineers concerned with structural applications (4).

1. Fiber

Composite materials formed by aligning extremely strong and stiff continuous fibers in a polymer resin matrix or binder have exceptional mechanical properties and are often termed advanced composites to distinguish them from chopped-fiber or otherwise filled polymers. The fibers that dominate the field of advanced composites are, in order of chronological development, S-glass, boron on a tungsten filament core, graphite or carbon, and aromatic polyamides (5). These fibers possess the desirable properties of low density (1.44-2.7 g/cm^3) and extremely high strengths (3-4.5 GPa) and moduli (80-550 GPa) (6).

High-performance carbon fibers have some physical properties which make them versatile materials for many applications. These carbon fibers are elastic to failure at normal temperature, which renders them creep-resistant and nonsusceptible to fatigue. They are chemically inert except in strong oxidizing environments or when in contact with certain molten metals. Also carbon fibers have exceptional thermophysical properties and excellent damping characteristics. However, carbon fibers are also brittle, have a low impact resistance, low break extension, and very small coefficients of linear expansion. They are expensive materials and can therefore be used only where cost is not a major factor. However, the price of these fibers is likely to decrease with increased production (7).

Carbon fibers are manufactured by spinning into fiber form a precursor material, the most common of which is polyacrylonitrile (PAN), oxidation of the fiber at 200-300°C, and carbonization of the fiber at 1000-2500°C in an inert atmosphere, surface treatment, and sizing. Diefendorf and coworkers (8-9) have outlined the synthesis of carbon fibers from PAN. Oberlin and Oberlin reported a particularly excellent overall study of the structure of carbon fibers (10).

2. Matrix

The other major constituent in fiber composites, the matrix, serves many important functions. It maintains the desired fiber orientations and spacings, protects the fiber from surface damage and under an applied force it deforms and distributes the stress to the high-modulus fibrous constituent (6). Several types of matrix materials such as glass, ceramics, metals and plastics have been used as matrices for reinforcement by carbon fibers. The thermosetting resins most commonly used are epoxies or modified epoxies, because of low density, beneficial mechanical properties and good fiber-matrix cohesion. Other thermosetting resins such as polyesters, vinyl esters and phenolics are also used because they are easier to handle than epoxies, although they are generally lower in mechanical performance. Several high-temperature polymer systems such as polyimides, bis-maleimides

and Friedel-Crafts products have now been developed which may improve the temperature range of application of these composites. Thermoplastic polymers, such as polyether sulfone, polyether ether ketone, polyphenylene sulfide and polyetherimide, offer considerable potential for the development of high performance thermoplastic composites due to their performance and processability (11).

3. Fiber-Matrix Relationship

The nature and the strength of the bond between the fiber reinforcement and the matrix has a strong influence on the overall mechanical performance of the composite material. It is essential to understand the adhesion which occurs at the fiber-matrix interface in order to efficiently utilize the properties of the fiber. Much recent work has emphasized the importance of fiber-matrix interaction (12-15).

4. Fabrication of Composites

Part of the attraction of composites is that many processes are available for their production. The processes may be grouped into two classes: open molding and closed molding. The main distinction is that open molds are one piece and use low or no pressure. Closed molds are two piece assemblies and can be used at higher pressures.

During fabrication, composite components are made against surfaces from which they must be released after the matrix has

cured. These surfaces are usually coated with release agents or a release cloth which contains release agents and is placed between the mold surface and the composite component. Release agents are commonly fluorinated polymers, silicones, and polyolefins (16) which may be transferred to the composite surface during fabrication of the composite.

B. High Temperature Structural Polymers and Adhesives

Natural adhesives have been used for many hundreds of years. However, synthetic adhesives were not widely used until the 1940s (17). One major group of adhesives used today are structural adhesives. A structural adhesive is a bonding agent used for transferring required loads between adherends exposed to service environments typical for the structure involved (18). A thermally stable or high temperature adhesive can be defined as a material which can withstand a given temperature range and can still retain its useful properties in a given application for a stated period of time (19).

High temperature structural adhesives play a major role in the aerospace industry. During the past two decades research into high-temperature polymers and adhesives has received extensive attention. Much of the progress in this field has been driven by the U.S. Government and the aerospace industries to achieve ever higher levels of thermal and structural performance. However, the development of

appropriate adhesives is lagging behind the production of structural aerospace materials. The U.S. government and aerospace industries have recognized specific adhesive needs generated by the development of advanced structural materials for elevated temperature applications on aircrafts and spacecrafts. Typical service lives for these materials can be expected to range from the single flight of a missile lasting for a few minutes at temperatures approaching 500°C to supersonic transport at temperatures ranging from 177° to 232°C for at least 50,000 hours (20).

The thermal and oxidative stability of organic polymers is improved by the incorporation of aromatic units such as benzene rings and heterocyclic rings, such as substituted imide, imidazole and thiazole, into the molecule. The most important resins currently available for use as adhesives in high temperature structural applications are the polyimides and polybenzimidazoles (21). Polyimides are formed by reaction of a diamine with a dianhydride and are superior to polybenzimidazoles for long-term strength retention (22).

Both linear-condensation and addition-type aromatic polyimides are materials under review as high temperature structural polymers and adhesives. Because of their toughness, flexibility, thermal and thermooxidative stability, radiation and solvent resistance, low density and excellent mechanical and electrical properties, linear aromatic

condensation polyimides are attractive candidates for aerospace adhesives.

Research on linear polyimide adhesives started in the 1960s (23). LaRC-TPI, a linear thermoplastic polyimide which can be processed in the imide form to produce large-area, void free adhesive bonds was developed in the late 1970's (24-26). LaRC-TPI is based on the 3,3'(m,m')-DABP and BTDA monomers shown in Figure 2.1 which shows the preparation of LaRC-TPI. Unlike conventional polyimides, LaRC-TPI is imidized and freed of water and solvent prior to bonding. Its thermoplastic nature is due to the structural flexibility introduced by bridging groups in the monomers and by the meta-linked diamine. LaRC-TPI has shown considerable potential as an adhesive because it allows the formation of large-area voidless bonds due to thermoplastic flow.

In order to alleviate the processing difficulties associated with high-temperature linear polyimides, addition-type polymers have been developed. Addition polyimides are easily processed in the form of short-chained oligomers which thermally chain extend by an addition polymerization involving unsaturated end groups. Although this method of polymerization alleviates the evolution and the problems associated with volatiles, the polyimides developed are thermosets which cure to form highly crosslinked networks. These crosslinked networks are very brittle in comparison to linear systems (20).

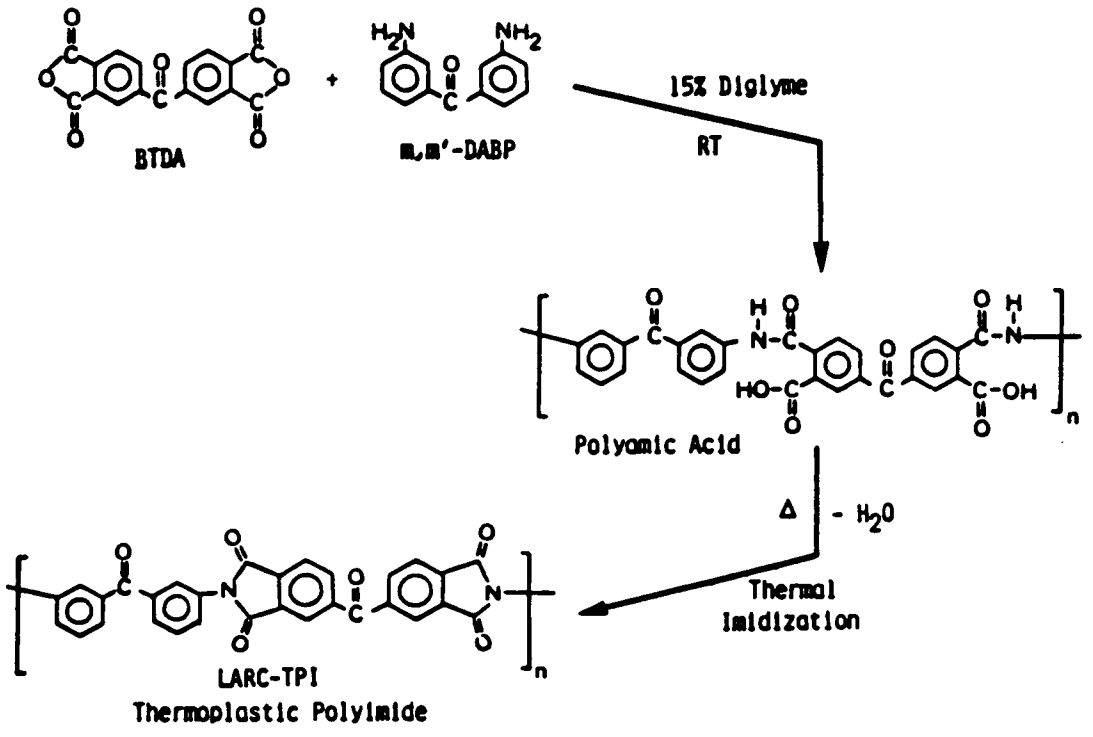

Figure 2.1. Preparation of LaRC-TPI polyimide adhesive (20).

LaRC-160 is an addition polyimide material based on the liquid monomers, diethylester of benzophenone tetracarboxylic acid (BTDE), the ethylester of norbornene dicarboxylic acid (NE) and Jeffamine AP-22, shown in Figure 2.2. LaRC-160 is an essentially "solventless" liquid resin which yields solventless drapable prepreg with good formability for the making of composites structures (28).

C. Adhesive Bonding

1. Adhesion Theories

Currently, there are four proposed mechanisms to explain the phenomenon of adhesion.

a. Mechanical Interlocking Theory

The mechanical interlocking theory attributes adhesion to the interlocking of the adhesive with irregularities, pores and roughness of the adherend surface. The most notable example is the adhesion of rubber to textile materials, where the bond strength was dependent on the penetration of fiber ends into the rubber (29). Packham's work on the adhesion of molten polyethylene to anodized aluminum indicated that an interlocking mechanism contributed significantly to the bond strength (30). However, the attainment of good adhesion between smooth surfaces, such as mica (31), clearly demonstrates that this theory is not of general applicability.

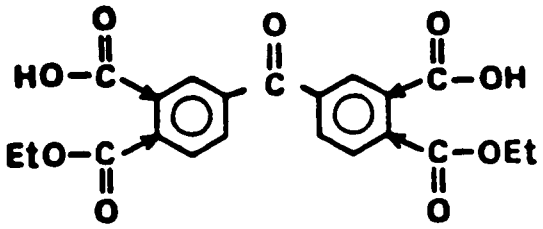

BTDE
MW = 414.4

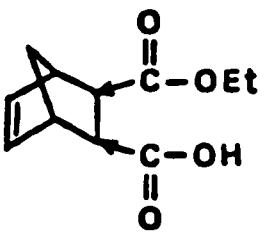

NE
MW = 210.2

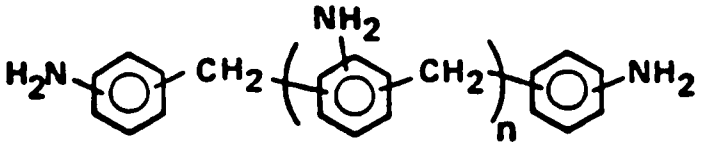

n = 0, 1, 2
Jeffamine AP-22
Avg. MW = 234

Figure 2.2. Monomers used in the preparation of LaRC-160 (27).

b. Diffusion Theory

The diffusion theory originally reported by Voyutskii (32), which deals specifically with polymer-polymer bonding, suggests that the long-chain polymer molecules or segments of these polymer molecules diffuse into each other, causing entanglements. The adherend and the adhesive must have fairly equal solubility parameters and the chains must be sufficiently mobile for at least limited diffusion. Voyutskii demonstrated that the peel strengths of pairs of polymers varied with the effective interdiffusion that occurred between the polymer pairs. The peel strengths of the polymer pairs varied with the bonding temperature and sharp increases in peel strengths corresponded with changes from interfacial to cohesive failure.

c. Electrostatic Theory

The electrostatic theory proposed by Derjaguin (33) states that a double layer of electrical charge exists at the interface of the adhesive and the adherend. Clear evidence exists that electrostatic forces are significant in considering adhesion between plane surfaces and particles (34,35). However controversy exists whether the electrostatic forces are a cause or merely a result of high joint strength.

d. Adsorption Theory

The adsorption theory states that adhesion results from molecular contact between two materials. The forces of attraction between the atoms in the two surfaces are varied in their nature and can be classified into two groups. Primary bonding includes covalent, ionic and metallic bonds at the interface. Primary bond strengths are on the order of 60 to 1200 kJ/mole. Studies which directly confirm primary bonding are scarce. Direct evidence has come through the introduction of small amounts (0.001-0.1 mole fraction) of reactive functional groups into the adhesive which often increases the adhesive bond strength (36). Specific functional groups may be selected for particular adherends where chemical bonding across the interface may be achieved. Also, the use of surface analytical techniques has produced definitive evidence that primary interfacial bonding occurs in certain circumstances (37-38).

The second group of forces of attraction, secondary bonding, includes permanent dipole-dipole interactions such as hydrogen bonding, acid-base interactions, dipole-induced dipole attractions and London dispersion forces. Secondary bond strengths are on the order of 0.01 to 42 kJ/mole. The forces which are important are dependent on the particular materials' chemistry. However, London dispersion forces are universally present and effective over a significantly greater distance (approximately 1 nm as opposed to 0.2 to 0.6 nm) than

the other forces mentioned above, such as primary bonding and hydrogen bonding. It has been calculated that the attractive forces between two infinite parallel plates is about 100 MPa at a separation of one nanometer. However the calculated theoretical values are much higher than the experimental strengths obtained which may be attributed to defects and air voids (39).

2. Bonding Configurations

Destructive mechanical tests are usually used to assess the performance of adhesive bonds. A large number of adhesive tests have been proposed and used. The analysis of various of these test methods is covered by Anderson et al. (40).

Three basic modes of failure can exist in adhesively bonded structures. As shown in Figure 2.3 opening or cleavage is mode I, in-plane shear or sliding is mode II, and sidewise shear or tearing caused by out-of-plane shear is mode III.

a. Single Lap Shear Test

Undoubtedly the most widely used adhesive test method is the single lap shear test. The requirements for this test are described by ASTM-01002 (42). The data obtained from this specimen, when used in conjunction with the Boeing wedge-crack test to verify the adequacy of the surface preparation, is quite useful for quality control and incoming receiving inspection (43). Some of the advantages of the single lap shear test are that the specimen geometry is simple and

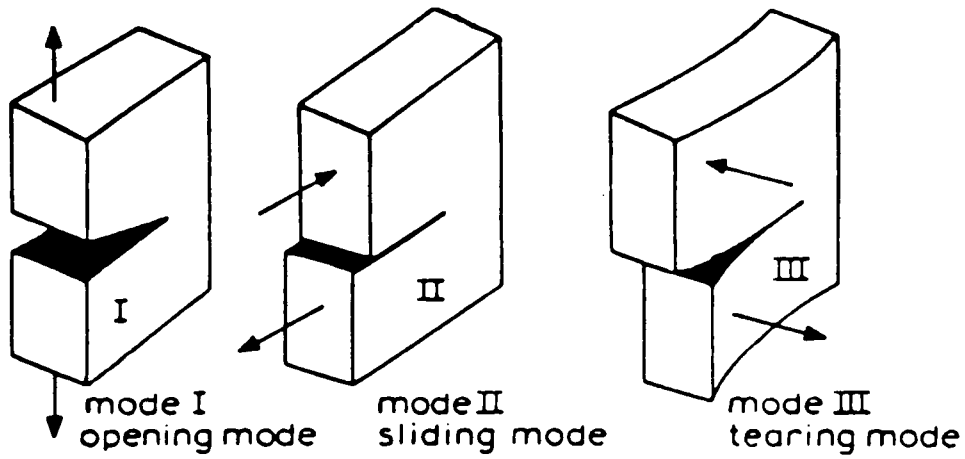

Figure 2.3. The three basic loading modes (41).

inexpensive to fabricate and test and that the only test apparatus required is a standard tensile testing machine. However the test has a number of disadvantages. The assumption that all loading is in the shear of the bond is incorrect because the single lap shear construction is asymmetric and application of a tension load causes a bending moment that deforms the test part. As a result stresses are concentrated at the edges of the bond. In addition these stresses are not constant throughout the thickness of the adhesive, but tend to concentrate near the re-entrant corners of the adherend. If the concentrated stresses exceed the yield strength of the adherend then the joint will deform so the applied force is no longer parallel to the plane of the bond and the bond will fail in a peel or cleavage mode beginning where the load is most concentrated at the edges (44). The stresses arising from the differential straining of this joint was first analyzed by Volkersen (45). The deformation of a single lap shear specimen and the distribution of shear stresses in a single lap shear specimen are shown in Figures 2.4 and 2.5, respectively.

b. Wedge Test

The wedge test or Boeing wedge test specimen developed by Marceau and coworkers (46) is a simplified, qualitative, less expensive version of the uniform double cantilever beam specimen. To determine the strain energy release rate, G_I,

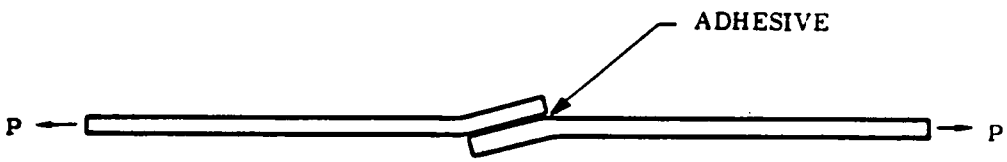

Figure 2.4. Deformation of the single lap shear specimen (40).

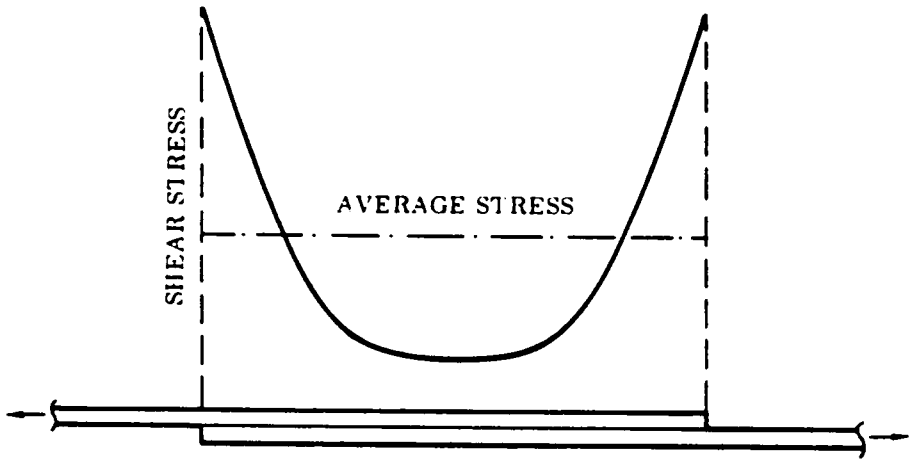

Figure 2.5. Shear stresses in a lap-shear specimen (40).

it is necessary to apply and measure a load placed on the sample for the double cantilever beam test, as opposed to only applying a constant displacement with the wedge test. The strain energy release rate can then be calculated for the wedge test by the equation

$$G_I = \frac{y^2 E h^3 (3(a + 0.6h)^2 + h^2)}{16\,((a + 0.6h)^3 + ah^2)^2} \qquad [2.1]$$

where y is the displacement at loadpoint, E is the adherend modulus, h is the thickness of the adherend and a is the crack length from the load point (46). The wedge test is a mode I environmental test which is capable of discriminating between adequate, marginal and inadequate surface preparation in various environments. This is achieved by driving a wedge into the bondline and measuring the initial crack length a_o. The specimen is then exposed to the desired environment, and the propagation of the crack is measured as a function of time. Typical plots of both a poor bond and a durable bond are shown in Figure 2.6. Depending on the rate of crack propagation, as well as the locus of failure at the crack tip, durability of the bonded joint may be assessed qualitatively. The wedge test is primarily used in this qualitative manner. Kennedy et al. used the wedge test to estimate the effect of different surface pretreatments on joint durability of titanium alloys bonded with an epoxy (48).

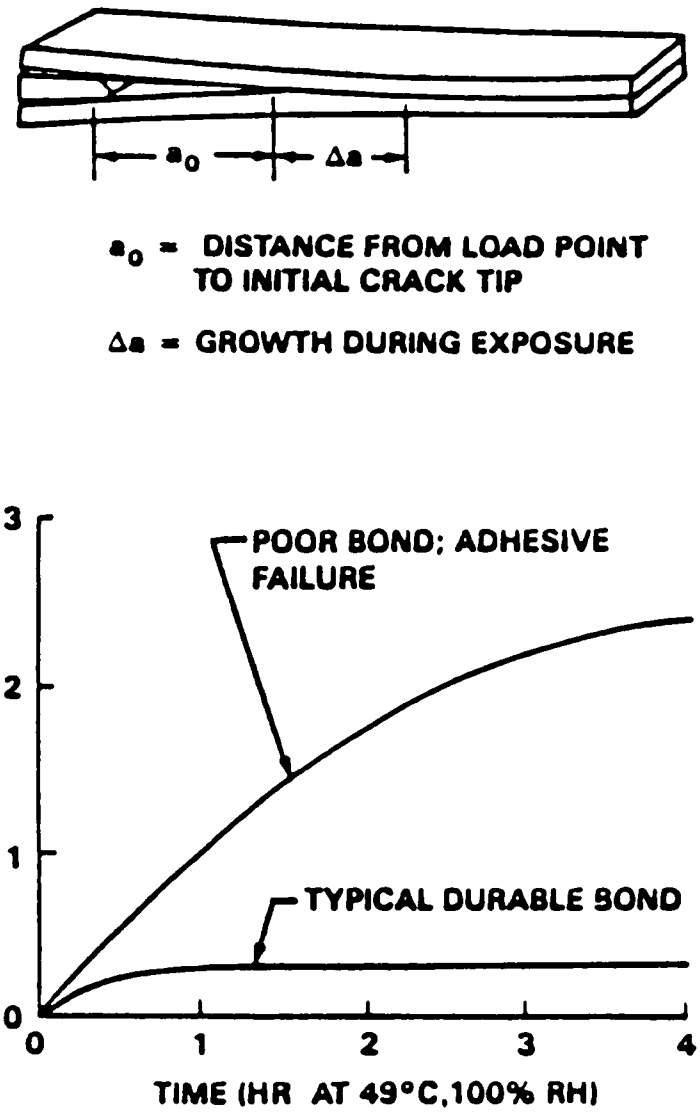

Figure 2.6. Change in crack length vs. time for a typical durable bond and a typical poor bond for the wedge test (47).

3. Surface Pretreatment

Surface preparation of adherends for adhesive bonding has been realized by the adhesion community to be a dominant factor in the performance and reliability of adhesively bonded components. Wightman and coworkers have demonstrated the importance of surface studies in adhesively bonded systems (49-52).

Surface pretreatments are used to develop an adherend surface to optimize the bonding at the adherend-adhesive interface. This may be done by the removal of a weak boundary which can reduce bond strength, as proposed by Bickerman (53). Weak boundary layers may include weak oxide layers for metals, low molecular weight species, release agents, and organic contamination. Surface treatments may also modify the physical structure of the adherend surface, which can play an important role if mechanical interlocking is one of the adhesion mechanisms of the system. Finally, preparation of the adherend surface can generate specific changes in the chemical nature of the surface to optimize adsorption interactions at the adhesive-adherend interface.

Chemical treatments, abrading, solvent cleaning, vapor degreasing, gritblasting, corona discharge and plasma treatments are some of the pretreatments commonly used today.

a. Plasma Pretreatment

A plasma is a system composed of radicals, excited molecules and atoms, ions and electrons. Cold plasmas and hybrid plasmas are the two types of plasmas mainly used. Cold plasmas are created when a gas under reduced pressure is subjected to a source of excitation, such as radio frequency. In a cold plasma the electron temperature is much greater, at least 10-100 times, than the gas temperature, which provides sufficient energy to cause disruption of molecular bonds. Hybrid plasmas are produced by corona discharges at atmospheric pressure (54).

Plasma treatments have been widely used to improve both the wettability and bondability of many polymers. The polymer radicals formed during the treatments are long-lived and can react with molecules in the air upon exposure after treatments. Therefore, even when an inert gas is used in the plasma treatment, introduction of polar group such as oxygen can be incorporated into polymer surfaces (55,56).

Numerous studies have demonstrated that since polar groups are always incorporated onto polymer surfaces, even when an inert gas is used, wettability of the polymers are improved (57-66). The extent of wettability improvement depends on specimen position, discharge power and frequency, treatment time, gas pressure and type, as well as other factors (62,67). Wettability can be very important in adhesion and can affect it in two ways. Incomplete wetting

produces interfacial defects, lowering the adhesive bond strength. Secondly, better wetting can increase adhesive bond strength by increasing the work of adhesion which has shown to be directly proportional to the fracture energy of a bond (68).

Both autohesive and adhesive bondabilities have been shown to be greatly increased with the use of plasmas (65,67-74). However, diverse views exist as to the mechanisms of bondability improvement. Improved wettability due to incorporation of polar groups (59,60,75-78), strengthening of the weak boundary layer (58,79), and hydrogen bonding (63,66,80) are but a few of the proposed mechanisms.

b. Effect of Surface Pretreatment on Composite-Composite Bonding

Although research in the area of composite-composite bonding is several decades old, the effect of surface pretreatment on composite-composite bonding has only been examined for the past fifteen years (50,81-89). Solvent washing or wiping and gritblasting or abrading are the most common composite pretreatments used today.

Several studies have shown that contamination of composite surfaces by release agents can reduce the strength of an adhesive joint (50,82-87). Gritblasting or abrasion of composite surfaces has been shown to increase adhesive bond strengths by reducing the levels of release agent

contamination (82-84,87). Matienzo et al. attributed increased bond strengths to not only decreased levels of contamination but also to roughening of the surface which may provide mechanical interlocking (86). Increased bond strengths have also been attributed to no air entrapment occurring during curing due to roughening of the composite surface which possibly provides a way for air to escape (81).

More recent work in the area of composite-composite bonding has demonstrated that chemical modification of composite surfaces by acid etching, plasma etching and corona-discharge pretreatments increase adhesive bond strengths and the fracture energy, G_c, of adhesively bonded composite joints by introducing specific functional groups on the surface (88-89).

III: EXPERIMENTAL

A. Materials

Five composite panels made from Celion 6000 carbon fibers with an NR 150 B2 polyimide finish in a LaRC-160 polyimide (see Figure 2.2) matrix were obtained from personnel at the NASA-Langley Research Center. One 16 ply composite panel was made at the NASA-Langley Research Center with a ply orientation of $[0_5/\pm 30/0]_s$. The other four composite panels were 14 ply panels with a ply orientation of $[0_3/\pm 30_2]_s$ and were made at Rockwell International. Details of the fabrication process have been previously reported (90).

The adhesive and primer used was LaRC-TPI (Langley Research Center - Thermoplastic Imide - see Figure 2.1) made by Mitsui Toatsui Chemicals (New York, New York) and was provided by personnel at the NASA-Langley Research Center.

The scrim cloth used was 112 E-glass cloth with an A-1100 (γ -aminopropylsilane) finish made by Burlington Glass Fabrics Company (Greensboro, North Carolina) and was provided by personnel at the NASA-Langley Research Center.

The argon, nitrogen and oxygen gases were obtained from Airco, Inc. (Radford, Virginia). The argon gas consisted of 99.995% argon, 2 ppm He, 10 ppm N_2, 2 ppm O_2, 2 ppm CO_2 and 10 ppm H_2. The prepurified nitrogen gas consisted of 99.998% nitrogen, < 35 ppm Ar, < 2 ppm He, < 5 ppm O_2, < 0.5 ppm CO_2 and < 10 ppm H_2. The oxygen gas consisted of 99.95%

oxygen, 0.29% Ar, 1/100 ppm N_2, 3 ppm CO_2 and 3 ppm H_2. The ammonia gas was obtained from Matheson Gas Products (East Rutherford, New Jersey) and contained 99.999% minimum ammonia, < 1 ppm CO_2, < 3 ppm N_2, < 5 ppm O_2 and H_2O and < 1 ppm CH_4.

The 2-methoxyethyl ether, $(CH_3OCH_2CH_2)_2O$, also commonly referred to as diglyme, was obtained from the Aldrich Chemical Company, Inc. (Milwaukee, Wisconsin). The Pd-Pt alloy was obtained from Ernest B. Fullam, Inc. (Lathem, New York). All other chemicals were obtained from Fisher Scientific Company.

B. Adhesive Tape Preparation

The adhesive tape was prepared by brush-coating the LaRC-TPI polyamic acid [7.5 wt.% solids in diglyme for the first two coats and 24.1 wt.% solids in diglyme for the following coats] onto 112 E-glass cloth with an A-1100 finish prior to coating. The glass cloth was tightly mounted on a metal frame and was oven dried for 30 minutes at 100°C. The 0.1 mm (0.004 in) thick glass cloth served as a carrier for the adhesive as well as for bondline thickness control and an escape channel for solvent. Coatings of the polymer solution were applied to the glass cloth until a thickness of 0.25-0.30 mm (0.010-0.012 in.) was obtained. After application of each coat, the adhesive tape was air-dried for 1 hour, placed in a forced-air oven for 1 hour at 100°C, 2 hours at 150°C and 3 hours at 175°C. The procedure used to prepare the tape was required to drive off the solvent and the reaction product volatiles

when converting the polyamic acid resin to the polyimide. Imidization of the polyamic acids to polyimides generally occurs in the 160°C range, with the degree of conversion being a function of time and temperature [91].

C. Composite Surface Pretreatments

The composite adherends were pretreated by five methods prior to analysis or adhesive bonding: 1) as-received 2) methanol wash, 3) methanol wash and sulfuric acid soak 4) gritblast and methanol wash 5) methanol wash and plasma discharge for various periods of time (0.5, 1, 2, 5, 10 or 20 minutes). The details of the procedures for the above pretreatments follow:

1. Methanol Wash - The composite was scrubbed on both sides with methanol using a natural bristle brush and then rinsed with methanol. The sample was then placed in a 130°C oven for 24 hours.

2. Sulfuric Acid Soak - The composite was soaked for 30 minutes in a 50/50 (by volume) solution of concentrated sulfuric acid and 30% H_2O_2 at room temperature. The sample was then rinsed three times with deionized water and blown dry with prepurified nitrogen.

3. Gritblast - Composites were gritblasted with 3 passes of the Econoline gritblaster gun held approximately 15 cm away from the sample, using silicon carbide #150 grit, at 60 psi.

4. Plasma - A Tegal Plasmod^{R} was used to produce a radio frequency (13.56 MHz) generated 50 watt plasma of ammonia, argon, oxygen or nitrogen. Pressure inside the chamber was 1.2 torr and the temperature was between 50^{o}C and 100^{o}C (92).

D. Instrumental Techniques

1. X-ray Photoelectron Spectroscopy (XPS)

XPS was used to determine the chemical composition of the composite panels following the surface pretreatments. In addition, after adhesive bonds had been tested, the failure surfaces were analyzed by XPS to determine the locus of failure.

XPS analysis was performed on a Perkin-Elmer PHI 5300 spectrometer employing a MgKα (1253.6 eV) achromatic X-ray source operated at 14 keV and an emission current of 20 mA. The vacuum was maintained at $< 2 \times 10^{-7}$ torr during analysis. Samples were approximately 1 x 2 cm and were mounted on the sample holder with double-sided tape. Analyses were obtained from a surface area of 2 x 10 mm. A PHI 10-360 hemispherical energy analyzer was used which operated in the constant pass energy (E_o) mode, where E_o = 44.75 eV for survey scans and E_o = 17.9 eV for high resolution narrow scans. Survey scans were taken from 0 to 1000 eV and narrow scans were obtained on any significant peaks observed in the survey scan spectra.

Samples were neutralized using a custom neutralizer attachment.

The as-received sample was analyzed using XPS and then analyzed again after it was methanol washed. All other samples were analyzed using XPS after the methanol wash procedure and then after the pretreatment. The oxygen plasma series was performed on the same sample with the noted time being the total time the sample had been exposed to the plasma. The binding energy of each photopeak was referenced to C 1s at 285 eV. For data evaluation the Perkin-Elmer 7500 computer (PHI software version 1.8) was used to obtain peak areas. Quantification of surface composition from XPS peak areas, A_i, was performed using the following equation:

$$CA_i = \frac{A_i}{\sigma_i} \frac{KE_i}{\lambda_i} \qquad [3.1]$$

where CA_i is the corrected area for the element, KE is the kinetic energy of the ejected photoelectron, σ is the cross-section calculated by Scofield (93) and λ is the mean free path, taken as $(KE)^{0.75}$. The corrected area is calculated for each element detected on the sample. The atomic fraction is obtained by ratioing the corrected area to the sum of the corrected areas for all elements detected.

2. Ion Scattering Spectroscopy (ISS)

ISS was used to determine the chemical composition of the pretreated composite adherends. ISS analysis was done on a Perkin-Elmer PHI 5300 spectrometer with an ISS attachment.

^{3}He ions were used at a scattering angle of 123^o. Survey scans were taken from 0.3 to 0.8 for the scattering ion energy ratio. Samples were neutralized and mounted in the same manner as for XPS. For data evaluation the Perkin-Elmer 7500 computer (PHI software version 1.8) was used to obtain peak areas. The atomic percentages were calculated by obtaining the areas under each peak and ratioing to the total peak area. No sensitivity corrections were made.

3. High Resolution Scanning Electron Microscopy (HR-SEM)

The surface topography of the pretreated composite adherends was examined using HR-SEM. Pretreated samples were sputter-coated with approximately 7 to 10 nm of a Pd-Pt alloy to reduce the effect of charging of the sample by the electron beam. Properly deposited the Pd-Pt layer does not alter the morphology within the resolution of the microscope. A Philips EM-420T STEM system at a beam voltage of 40 kV was used to take the photomicrographs.

4. Photoacoustic Fourier Transform Infrared Spectroscopy (PAS-FTIR)

A Nicolet 5DXB spectrometer with a MTEC 100 photoacoustic cell and detector was used to analyze 0.9 cm disks of the pretreated composites. The photoacoustic sample chamber was purged with helium for 5 minutes. The spectrometer bench was purged with dry nitrogen for 30 minutes prior to analysis.

One hundred co-added interferograms were scanned at 4 cm^{-1} resolution. A spectrum from 4000 to 400 cm^{-1} was obtained against a background reference of Norit A alkaline decolorizing carbon black.

5. Contact Angle Measurements

To determine the wettability of the pretreated composite surfaces, contact angle measurements were obtained. Ten μl deionized water drops and six μl diglyme drops were placed on the composite surfaces using a syringe held approximately 3 mm above the surface. The sessile contact angle of the drop was measured by a Rame-Hart #100-00 115 NRL goniometer telescope. The left and right side of at least three drops for each liquid were measured for each pretreatment.

E. Adhesive Bonding

1. Priming Procedure

The LaRC-TPI primer used was 20 wt% solids in diglyme. A thin coat of primer was applied with a brush to all composite samples immediately after pretreatment. Samples were then placed in an oven for 30 minutes at 60°C, 15 minutes at 100°C and 15 minutes for 150°C. Samples were allowed to cool to room temperature and then were placed in a desiccator until bonding.

2. Single Lap Shear Test

Lap shear coupons (10.16 x 2.54 cm) were pretreated, primed and bonded with one layer of the LaRC-TPI adhesive tape. The lap shear coupons were placed in a jig set for 1.27 x 2.54 cm overlap. The jig was placed in a Carver Laboratory Model C press and heated from room temperature to 316°C (600°F) at 50 psi bonding pressure for 2 hours. The heat was turned off and the joints allowed to cool to room temperature under pressure. All lap shear joints were placed in one of three environments: (i) room temperature, desiccator, 1000 hours, (ii) forced-air oven, 204°C, 1000 hours and (iii) immersion in boiling deionized water, 3 days. After environmental aging, lap shear bonds were pulled to break at room temperature on an Instron testing machine at a cross head rate of 0.127 cm/min. The failure surfaces were studied by XPS to determine the locus of failure.

3. Wedge Test

Wedge coupons (2.54 x 12.7 cm) were pretreated, primed and bonded with one layer of LaRC-TPI cut to the same dimensions as the wedge coupons leaving 1 cm clear at each end. All bonding conditions were identical to the lap shear bonding conditions stated above, except that no jig was used to prepare the wedge joints. After the wedge samples were removed from the press, a 0.38 cm thick Ti 6Al-4V wedge was slowly driven into one end of the wedge joint at a distance

of 1.5 cm, with the use of a vise, causing an initial crack to propagate. The position of the initial crack was measured with a ruler to the nearest 1 mm and the joint was placed in one of three environments: (i) room temperature, desiccator, 1000 hours, (ii) forced-air oven, 204°C, 1000 hours and (iii) immersion in boiling deionized water until total debonding of the wedge sample. The crack propagation with time was then determined periodically by removing the joint from the environment to measure the crack. The failure surfaces were examined by XPS to determine the locus of failure.

F. Statistical Analysis

1. Standard Deviation

Data from the contact angle measurements, the wedge test and the single lap shear test were analyzed statistically to determine the variability of the measurements. All measurements are reported as $\bar{x} \pm s$, where $\bar{x}$ is the average value and s is one standard deviation for a small number of measurements. The value of s, was calculated by

$$s = \left[\frac{\sum_{i=1}^{N} (x_i - \bar{x})^2}{N-1} \right]^{1/2} \qquad [3.2]$$

where N equals the number of measurements and x_i is the specific measurement.

2. Analysis of Variance

Data from the wedge test and the single lap shear test were also analyzed statistically to determine if a distinction exists between various populations on the basis of their mean values. In this particular study, a population will consist of data obtained from the same surface pretreatment. Testing the equality of three or more population means can be accomplished by the use of analysis of variance which is considered to be one of the most widely used and powerful statistical techniques (94). Analysis of variance, also commonly referred to as ANOVA, is the process of subdividing the total variability of experimental observations into portions attributable to recognized sources of variation. The analysis of variance determines if there are definite statistical differences between the populations, through the testing of the equality of the population or pretreatment means. That is the test of

H_o: all treatment means are equal which is equivalent to

$$H_o: \mu_1 = \mu_2 = \ldots = \mu_k$$

where Ho is the null hypothesis, the statement subjected to the test procedure, and μ_i is the population mean value.

The population mean square, MSp, measures the variation among the sample treatment means and is based on the term

$$\sum_{i=1}^{k} n_i \, (\bar{x}_i - \bar{\bar{x}})^2 \qquad [3.3]$$

where n_i is the number of measurements for the ith population, $\bar{x}_i$ is the mean value for the ith population and $\bar{x}$ is the mean value for all the populations. The residual mean square, MS_R, measures the variability within population groups and is based on the term

$$\sum_{i,j} (x_{ij} - \bar{x}_i)^2 \qquad [3.4]$$

where x_{ij} is the jth observation obtained from the ith population.

It can be concluded that significant differences exist among the population means if the value of MS_p is considerably larger than MS_R; that is if the variation among the sample population means is larger than the within group variability. Therefore the ratio MS_p/MS_R, which is also referred to as the F value or F distribution, is the statistic for testing H_o. More specifically, the critical or accepted region for this F value must be larger than an F distribution with k-1 numerator and n-k denominator degrees of freedom, $F_{k-1,n-k}$. This $F_{k-1,n-k}$ value may be obtained from an F-Distribution table for a chosen level (95). Therefore, the null hypothesis, H_o, is rejected if $F \geq F_{k-1,n-k}$ for a chosen F-distribution level (94). All data was evaluated through the use of the Statistical Analysis System (SAS), developed by the SAS Institute Inc., (Cary, North Carolina) and a 5 percent F-distribution level was chosen for all analyses.

3. Multiple Comparisons

Analysis of variance determines if significant differences among the population means exist. A significant result in analysis of variance can arise for several reasons. Some of these reasons can be that one mean may differ from all the others, all the means may differ from each other, or the means may fall into distinct groups. However, to determine the magnitude of the differences or where the differences occur, other procedures such as multiple comparison procedures must be employed. One way of deciding if a significant result exists is to arrange the means in order of increasing size and then compare the difference between adjacent values with a predetermined quantity of significant differences (96, 97). The Least Significant Difference (LSD), and Duncan's Multiple-Range Test are two commonly used multiple comparison tests and were the multiple comparison tests chosen for all analyses with the use of SAS.

IV. RESULTS AND DISCUSSION

A. Characterization of Pretreated Composite Surfaces

1. Chemical Composition

As discussed in the LITERATURE REVIEW section, surface pretreatment is a very important factor in adhesive bonding. The objective of this section was to characterize the composite surfaces before and after pretreatment in order to obtain a better understanding of the role that surface pretreatment has on adhesive bond strength and durability.

a. XPS

Surface pretreatment may affect the chemical composition of composite surfaces. The results presented in this section are aimed at understanding changes in the chemical composition of the composite surfaces before and after surface pretreatment.

The purpose of the XPS surface analysis was to examine composite surfaces before and after pretreatment to identify and quantify the elements present in the surface. With XPS, the exact element location on the surface is not possible since the signal is averaged over a large area (2 x 10 mm). XPS analyses are confined to the top 5-10 nm of the surface analyzed and are sensitive to approximately a one percent concentration of an element. XPS analysis is widely used in the areas of research concerning interfaces and surfaces and

it is an invaluable tool because of the range of sample types which can be examined.

The calculated atomic percentages are listed in Table 4.1 for each element in all samples before and after the specified surface pretreatment. As expected, carbon is the major atomic constituent present in approximately the top 5-10 nm of the composite surface. The XPS spectra of the C 1s photopeaks are shown in Figure 4.1 For the gritblast sample (see Figure 4.1F), a shoulder to the right of the main -C-C- photopeak is present. An additional study was performed to identify this lower binding energy peak. Here, a gritblast sample was coated with 1 nm gold and then analyzed using XPS. The observed gold doublet ($4f_{5/2}$ and $4f_{7/2}$) peaks at 87.7 and 84.0 eV, respectively, were not the narrow, well resolved expected peaks. In fact, the observed peaks were broad indicating charging of the gritblast sample even though a neutralizing gun was used. This incomplete neutralization seems reasonable since gritblasting produced an extreme macro-roughening of the surface which was not seen for any other sample by HR-SEM. This macro-roughening of the gritblast surface could be the cause of the differential charging. Madeleine, et al. observed similar broad gold doublet peaks as a result of differential charging for polyimide films which have been modified by the incorporation of metal containing compounds (98).

TABLE 4.1

XPS results of pretreated composites.

Sample Number	Pretreatment	Atomic Concentration (%) C	O	N	F	Si	Na	S	Ca	Ar
1	As-received	46.5	12.4	2.0	36.3	1.9	0	0.9	trace	--
1	Methanol Wash	49.7	7.6	2.3	40.4	trace	0	trace	0	--
2	Methanol Wash	49.6	8.8	2.3	27.7	1.2	0	0.3	trace	--
2	Sulfuric Acid Soak	50.3	10.7	2.5	34.2	1.1	0	1.2	0	--
3	Methanol Wash	51.5	6.2	2.1	39.6	0	0	0.6	0	--
3	Gritblast	72.6	7.8	6.1	13.5	trace	0	0	0	--
4	Methanol Wash	50.9	9.0	2.4	36.8	0.9	0	trace	0	--
4	0.5 Min. Oxygen Plasma	41.8	19.1	2.7	33.6	1.8	trace	1.0	trace	--
4	1 Min. Oxygen Plasma	42.4	21.2	2.8	30.2	1.9	trace	0.9	trace	--
4	2 Min. Oxygen Plasma	46.2	31.5	4.2	12.9	3.1	0.6	1.6	trace	--
4	5 Min. Oxygen Plasma	50.8	36.8	2.4	0.8	3.2	2.5	2.6	0.9	--
4	10 Min. Oxygen Plasma	48.4	36.6	3.6	0.7	3.8	3.0	3.2	0.7	--
4	20 Min. Oxygen Plasma	50.1	35.4	3.6	0	3.6	3.2	3.2	0.8	--
5	Methanol Wash	49.9	7.0	2.6	39.7	0.8	0	trace	0	--
5	5 Min. Nitrogen Plasma	42.3	13.6	2.9	39.1	1.2	0.3	0.6	0	--
6	Methanol Wash	51.6	6.9	1.8	38.5	0.9	0	0.3	0	0
6	5 Min. Argon Plasma	54.0	22.4	4.4	15.7	1.4	0.4	0.9	0.8	trace
7	Methanol Wash	52.5	7.8	1.6	38.1	trace	0	trace	0	--
7	5 Min. Ammonia Plasma	49.0	7.9	5.2	37.4	0	0	0.5	0	--
8	Methanol Wash	51.8	9.0	1.6	37.6	0	0	0	0	0
8	7 Min. Argon Plasma followed by 5 min Ammonia Plasma	63.5	17.1	10.7	5.5	1.8	0.7	0.8	trace	trace

-- : element not determined

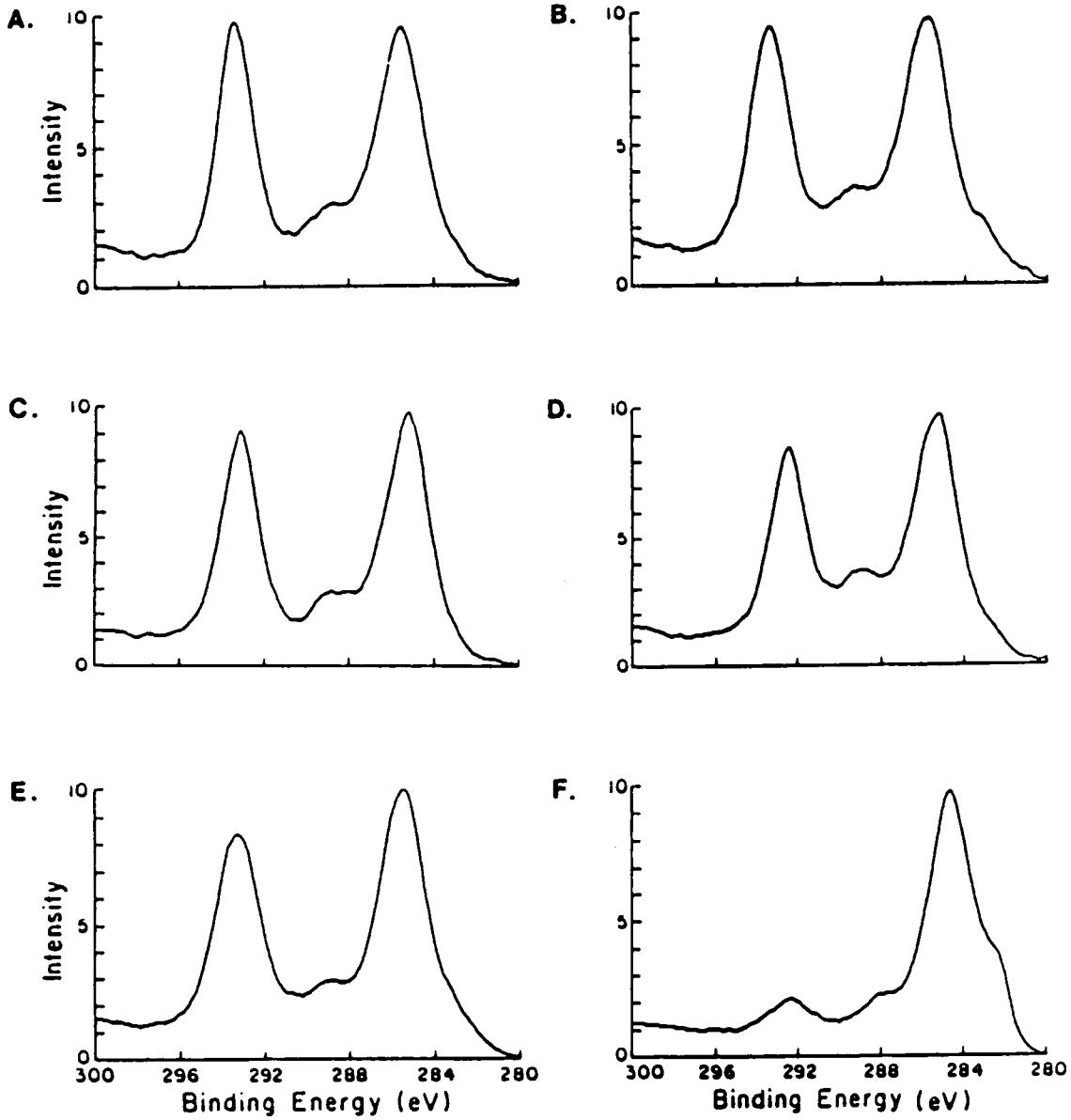

Figure 4.1. XPS spectra of C 1s photopeaks of pretreated composites. (A) As-received (B) Methanol wash (C) Methanol wash (D) Sulfuric acid soak (E) Methanol wash (F) Gritblast (G) Methanol wash (H) 0.5 min. oxygen plasma (I) 1 min. oxygen plasma (J) 2 min. oxygen plasma (K) 5 min. oxygen plasma (L) 10 min. oxygen plasma (M) 20 min. oxygen plasma (N) Methanol wash (O) 5 min. nitrogen plasma (P) Methanol wash (Q) 5 min. argon plasma (R) Methanol wash (S) 5 min. ammonia plasma (T) Methanol wash (U) 7 min. argon plasma followed by 5 min. ammonia plasma.

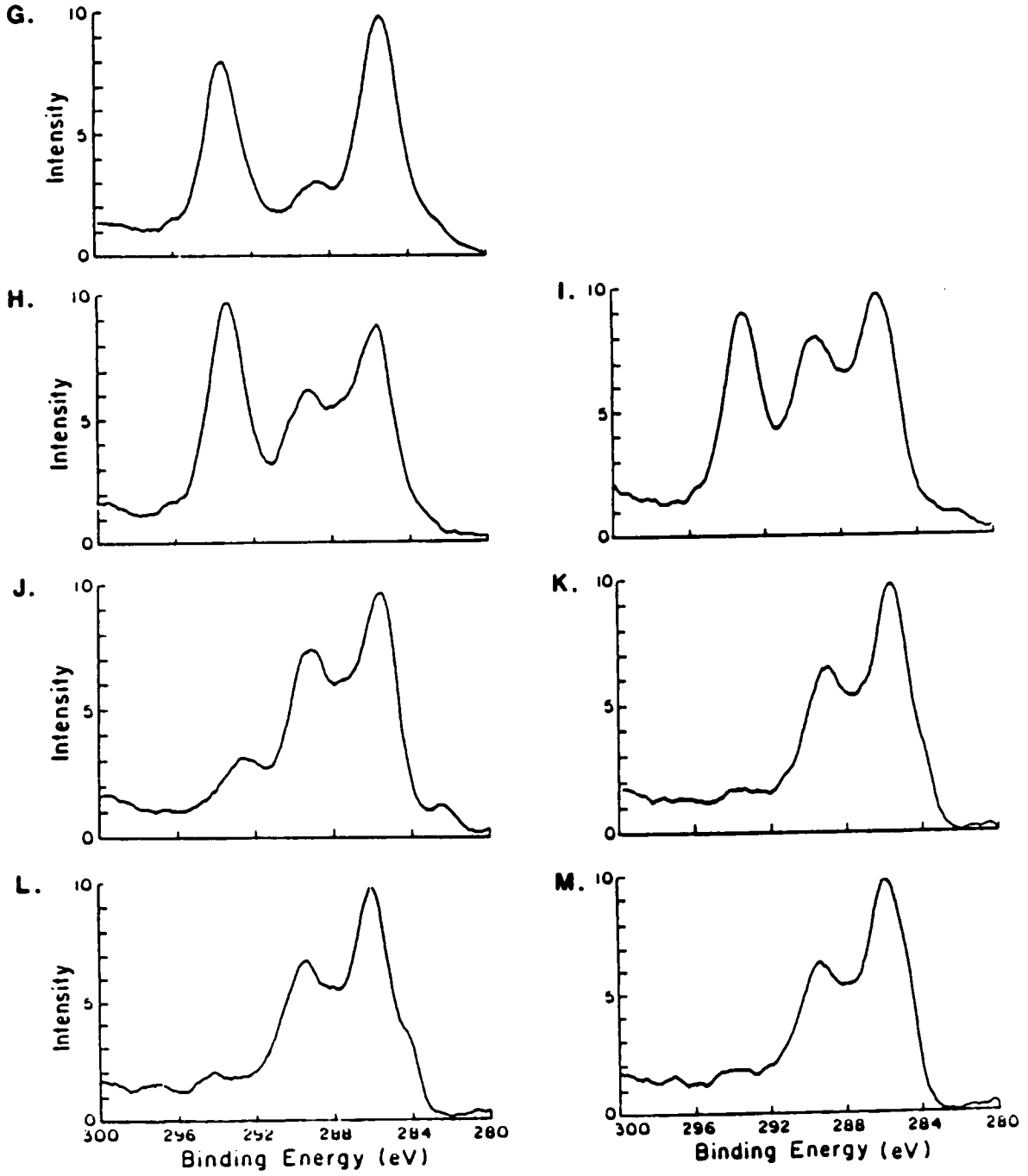

Figure 4.1 (continued).

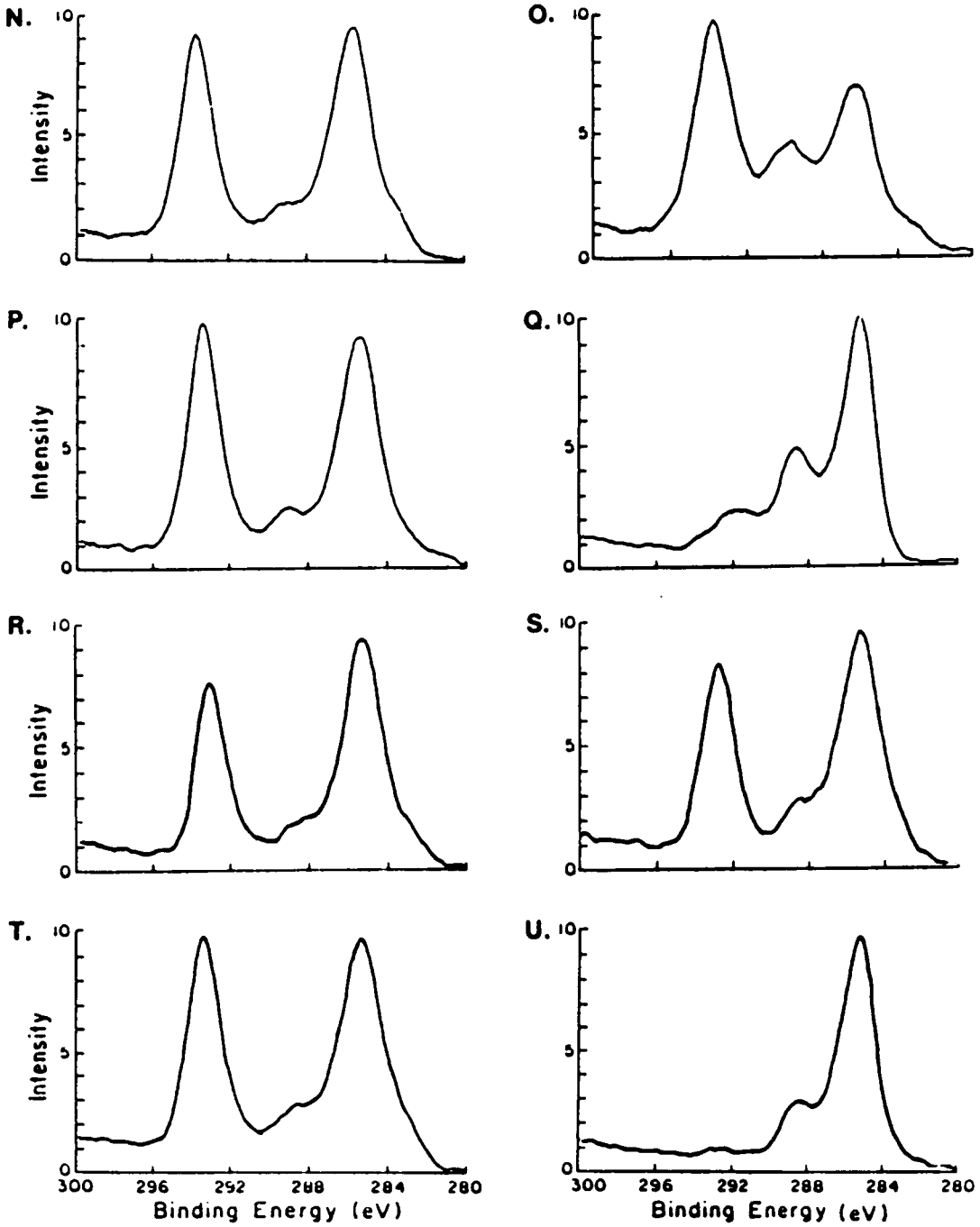

Figure 4.1 (continued).

A fluorocarbon peak was noted at approximately 293 eV for the as-received, all methanol washed, sulfuric acid soak, 5 minute ammonia plasma, and 0.5 and 1 minute oxygen plasma and 5 minute nitrogen plasma samples. The fluorocarbon is attributed to contamination from the release cloth used during the fabrication of the composite panel. In addition to release cloth contamination, it is well known that pretreated solid surfaces contaminate readily upon exposure to laboratory conditions. Koranyi and Acs reported that the contact boundary angle of distilled water on the surface of a cleaned plate of alkali lime silicate glass increased from near zero to 23^{o} due to the effect of air moisture and contaminants absorded from the atmosphere (99). However the type, extent and speed of contamination is not often documented particularly in adhesion studies. This paper contained in the appendix addresses the contamination of pretreated Ti 6Al-4V samples in a laboratory environment.

Almost total elimination of the fluorocarbon peak was observed for the gritblast, the 5 minute argon plasma, the 2,5,10 and 20 minute oxygen plasma and the 7 minute argon followed by a 5 minute ammonia plasma samples. The F 1s photopeak is discussed in more detail below. The detection of fluorocarbon on the composite surfaces is consistent with the earlier results of Messick, et al. who reported that the fluorocarbon is introduced as a result of contact of the composite with a Teflon coated glass fabric during the

fabrication of the composite (100). Brewis et al. (82), Stone (83), Parker and Waghorne (84), and Matienzo et al. (86) have all reported a reduction in joint strength due to the contamination of the composite surfaces by release agents. Parker and Waghorne (84) have reported almost a linear relationship between the concentration of surface organo-fluorine contamination and both the joint strength and the proportion of interfacial failure.

Peaks observed between the 285 and 293 eV peaks can be attributed to both carbon-oxygen and carbon-nitrogen containing functionalities. Increase in the intensity of peaks in this region is seen for samples which have been pretreated in 5 minute argon, 5 minute nitrogen, 7 minute argon followed by 5 minute ammonia and all oxygen plasmas. Definitive curve fitting of the spectral region is inappropriate due to the complexity of overlapping peaks. Further work using a technique such as selective chemical derivatization (101,102) of the surface followed by XPS analysis could be used to assign the peaks in this area. Increasing the number of carbon-oxygen and carbon-nitrogen functional groups may offer great potential for enhanced adhesive bonding with LaRC-TPI due to chemical reactions which might occur.

Possible reactions which could occur between the LaRC-TPI primer and the pretreated composite surfaces are shown in Figure 4.2. Primary amines, either from the LaRC-TPI primer

or which have been incorporated into the composite surface through ammonia plasma pretreatments, have the potential to react with carboxylic acid groups, either from the LaRC-TPI primer or which have been incorporated into the composite surface through argon, nitrogen or oxygen plasma pretreatments, to form an amide bond (see Figure 4.2A). Also primary amines have the potential to react with carbonyl groups, either from the LaRC-TPI primer or which have been incorporated into the composite surfaces through argon, nitrogen or oxygen plasma pretreatments, in a ketimine reaction (see Figure 4.2B) (103). Anhydride end groups, from either the LaRC-TPI primer or the LaRC-160 composite matrix, could also have the potential to bond with primary amines yielding an amide-acid and finally a polyimide (see Figure 4.2c). Hydroxyl groups which could have been incorporated into the composite by argon, nitrogen and oxygen plasma pretreatments, have the potential to react with anhydride and carbonyl groups in the LaRC-TPI primer (see Figure 4.2D and E). However the last two reactions are not very likely, especially in comparison to the three reactions stated above.

The oxygen content was essentially constant (6-12%) for each sample with the exception of the plasma pretreated samples. The amount of oxygen increased as the time the sample was placed in the oxygen plasma increased, with a plateau at around 35 percent occurring sometime after 2 minutes. An increase in oxygen was also found for the 5

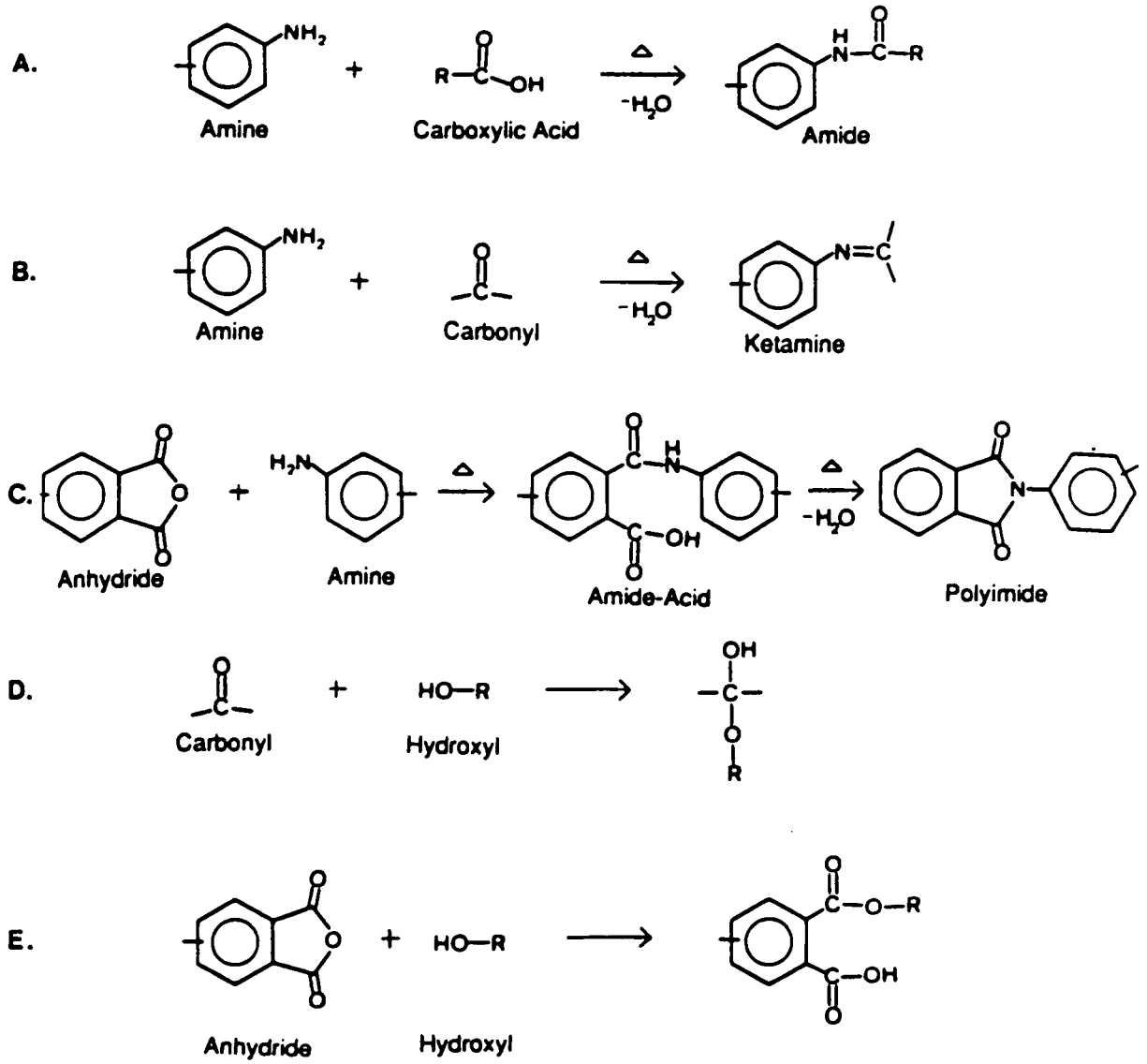

Figure 4.2. Possible reactions which could occur between the LaRC-TPI primer and the composite surfaces.

minute argon and nitrogen plasma treatments. This increase may be attributed to the fact that the samples which are extremely reactive after plasma pretreatment were exposed to the atmosphere immediately after treatment. Yasuda et al. (55) and Clark and Dilks (56) also reported that even when an inert gas was used in plasma pretreatments of polymers, introduction of polar groups such as oxygen, can be incorporated into the polymer surfaces due to polymer radicals formed during the treatments which are long-lived and can react with molecules in the air upon exposure after treatments.

Fluorine in varying amount was present for each of the samples except the 20 minute oxygen plasma samples as noted in Table 4.1. The high concentration of fluorocarbon on the as-received sample (36 atomic percent) is attributed to contamination transferred from the release cloth during the fabrication of the composite panel. As mentioned before, numerous studies have shown a reduction in bond strength due to contamination of the composite surfaces by release agents (50,82-87). The atomic amount of fluorine decreased as the time the sample was placed in the oxygen plasma increased. This trend is opposite to what was observed with oxygen. The largest change in fluorine concentration was observed between 1 and 2 minutes with almost complete removal of fluorine between 2 and 5 minutes.

There is an increase in the amount of nitrogen incorporated into the 5 minute ammonia plasma and 7 minute argon plasma followed by 5 minute ammonia plasma pretreated surfaces. For all other surface pretreatments, a consistent amount of nitrogen was observed which can be attributed to the nitrogen in the amine functionality found in the LaRC-160 polyimide matrix. The increase in the nitrogen due to the ammonia plasma pretreatment increases the area under this peak with no shifting in the binding energy of the peak. Therefore the increase in nitrogen incorporated into the ammonia plasma pretreated composite surfaces is due to an increase in amine functional groups. No nitrogen increase was observed even for composite samples exposed to a nitrogen plasma in contrast to the oxygen plasma. This result suggests that changes in the intensity of the photopeaks centered around 288 eV for 6 minute nitrogen, 5 minute argon, and all oxygen plasma pretreated composite surfaces are due to C-O and not C-N moieties.

Small amounts of silicon, sulfur, sodium and calcium were present on the various samples. Based on the binding energies of these elements the silicon peak at 103.5 eV can be attributed to silicon dioxide, SiO_2. Sulfur, with a binding energy of 169.3 eV can be attributed to a sulfate group, which may be found on the composite as sodium sulfate, Na_2SO_4, or calcium sulfate, $CaSO_4$. At 1071.6 eV, the sodium may be assigned to either sodium fluoride (NaF) or sodium sulfate

(Na_2SO_4). The binding energy of calcium was 348.0 eV which may be attributed to calcium fluoride (CaF_2) or calcium sulfate ($CaSO_4$). Silicon, sulfur and calcium were present on the as-received sample. Gritblasting was the only pretreatment which removed sulfur and calcium. All four contaminants were detected in small amounts for the oxygen and argon plasma pretreated samples while silicon, sulfur and sodium were present on the nitrogen plasma pretreated samples and only sulfur was detected on the ammonia plasma pretreated samples. Here, an additional source of silicon, sodium and calcium is probably the glass container in which the samples were placed while being plasma pretreated. These contaminants could have the potential to reduce bond strengths as shown by Parker who reported that various contaminants, including release agents and a number of substances which could be deposited on the surface of a composite component during handling and servicing, may interfere with adhesive bonding of composites (87).

b. ISS

The purpose of the ISS surface analysis was to examine the composite surfaces before and after pretreatment, to identify and quantify the surface elements for the entire surface. ISS analyses do not determine the exact element location on the surface. The ISS technique is sensitive to

approximately a one percent concentration of an element and samples a depth limited to the uppermost atomic layers.

The ISS survey spectra of the pretreated composite samples are shown in Figure 4.3. The intensity is plotted as a function of scattering ion energy to incident energy ratio, E(s)/E(o), in each case. Obvious differences are seen in the spectra for different pretreatments. These are the first reported ISS spectra of carbon fiber-polymer matrix composites. Peak positions for each element are reported in Table 4.2. The atomic percentages calculated from the ISS survey spectra are listed in Table 4.3. It is commonly accepted that the sampling depth of ISS is limited to the uppermost atomic layers (0.3-1 nm) whereas the XPS technique has a sampling depth of 5-10 nm. Hence, high concentrations of sodium and calcium observed on the oxygen plasma samples and the 7 minute argon plasma followed by 5 minute ammonia plasma, by ISS, in contrast to the lower concentrations observed in the XPS results (see Table 4.1) may be attributed to the change in sampling depth. Another reason why the sodium and calcium peaks may be so intense as compared to the other elements is because the ISS technique becomes increasingly sensitive to elements with higher atomic numbers as can be seen in Figure 4.4. It is interesting to note that the nitrogen and argon plasma treated samples do not contain detectable quantities of sodium and calcium. Therefore, these elements are transported much more rapidly in an oxygen plasma

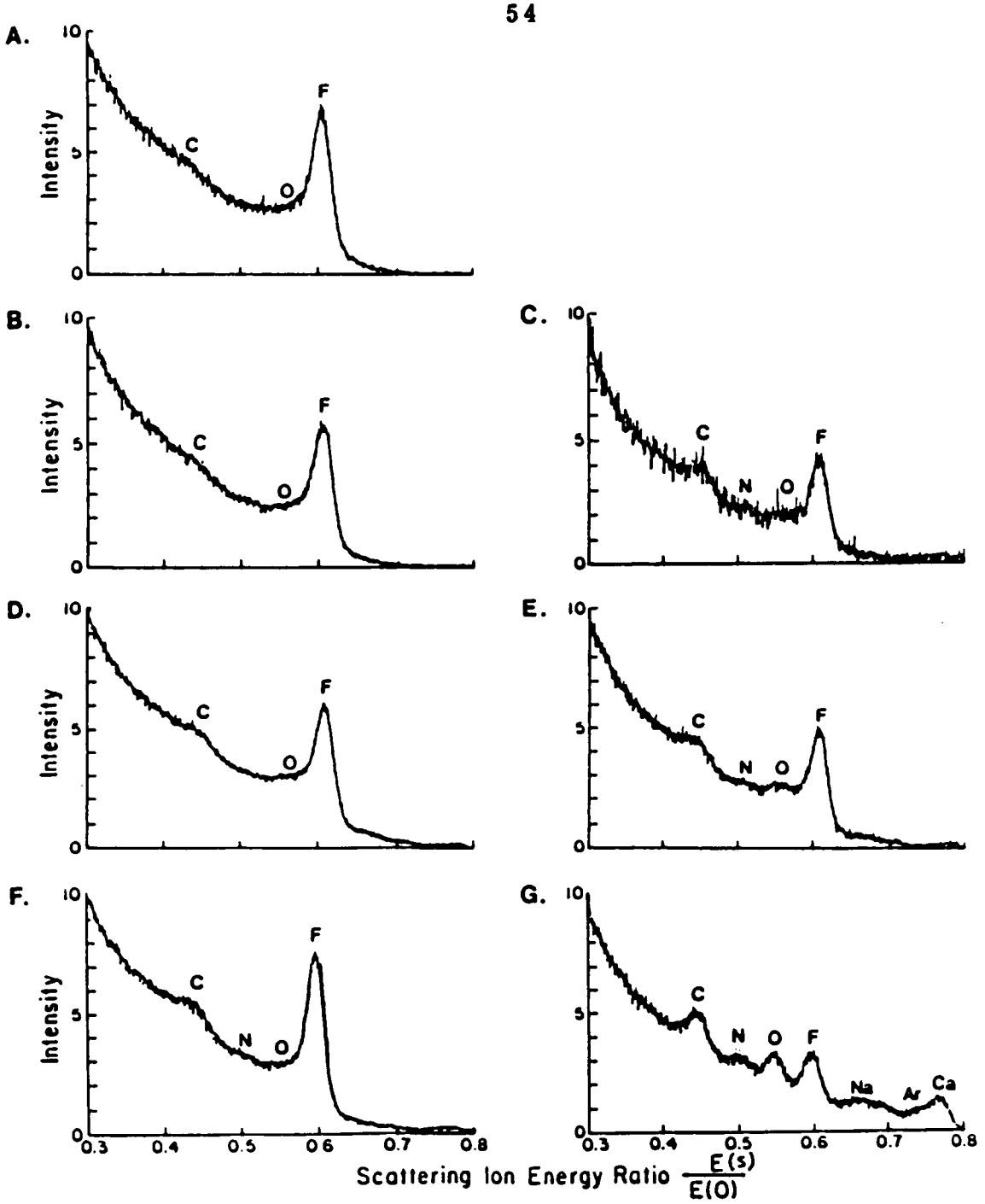

Figure 4.3. ISS survey spectra of pretreated composites. (A) Methanol wash (B) Sulfuric acid soak (C) Gritblast (D) 5 min. nitrogen plasma (E) 5 min. argon plasma (F) 5 min. ammonia plasma (G) 7 min. argon plasma followed by 5 min. ammonia plasma (H) 0.5 min. oxygen plasma (I) 1 min. oxygen plasma (J) 2 min. oxygen plasma (K) 5 min. oxygen plasma (L) 10 min. oxygen plasma (M) 20 min. oxygen plasma.

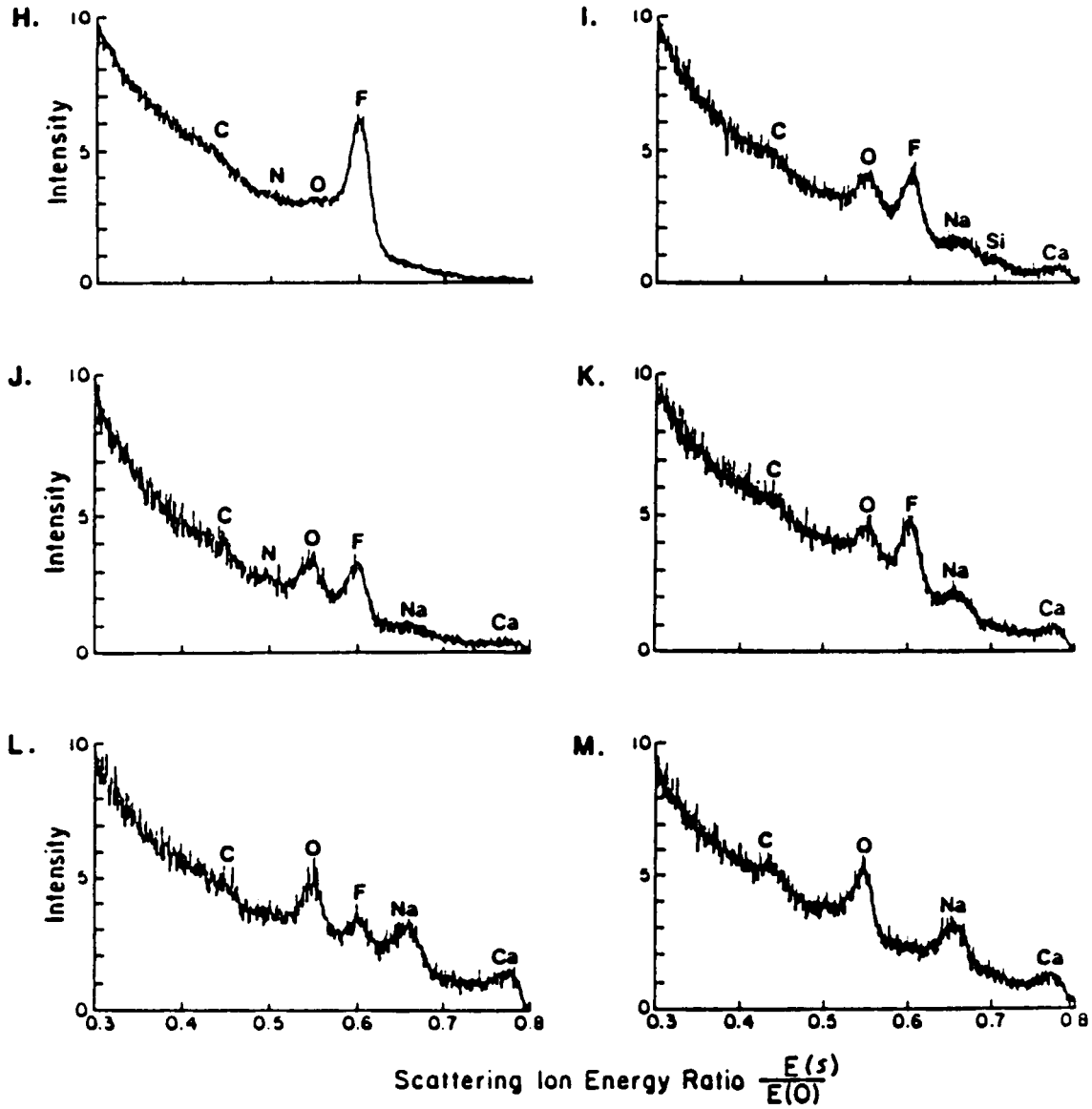

Figure 4.3 (continued).

TABLE 4.2

Scattering ion energy to incident energy ratios, E(s)/E(o), for ^{3}He.

Element	$\frac{E(s)}{E(o)}$
C	0.45
N	0.51
O	0.55
F	0.60
Na	0.66
Si	0.71
S	0.74
Ca	0.78
Ar	0.79

TABLE 4.3

ISS results of pretreated composites.

Pretreatment	Atomic Concentration (%) C	N	O	F	Na	Si	Ca	Ar
Methanol Wash	10.	0	5.	85.	0	0	0	0
Sulfuric Acid Soak	11.	4.	4.	81.	0	0	0	0
Gritblast	58.	5.	12.	26.	0	0	0	0
0.5 Min. Oxygen Plasma	12.	2.	8.	79.	0	0	0	0
1 Min. Oxygen Plasma	17.	trace	21.	38.	10.	5.	8.	0
2 Min. Oxygen Plasma	23.	4.	29.	35.	6.	trace	4.	0
5 Min. Oxygen Plasma	19.	trace	23.	36.	13.	0	9.	0
10 Min. Oxygen Plasma	20.	trace	28.	14.	24.	0	13.	0
20 Min. Oxygen Plasma	15.	6.	38.	0	28.	0	13.	0
5 Min. Nitrogen Plasma	13.	0	9.	78.	0	0	0	0
5 Min. Argon Plasma	17.	3.	11.	69.	0	0	0	0
5 Min. Ammonia Plasma	13.	7.	1.	79.	0	0	0	0
7 Min. Argon Plasma followed by 5 Min. Ammonia Plasma	21.	16.	7.	24.	11.	0	15.	5.

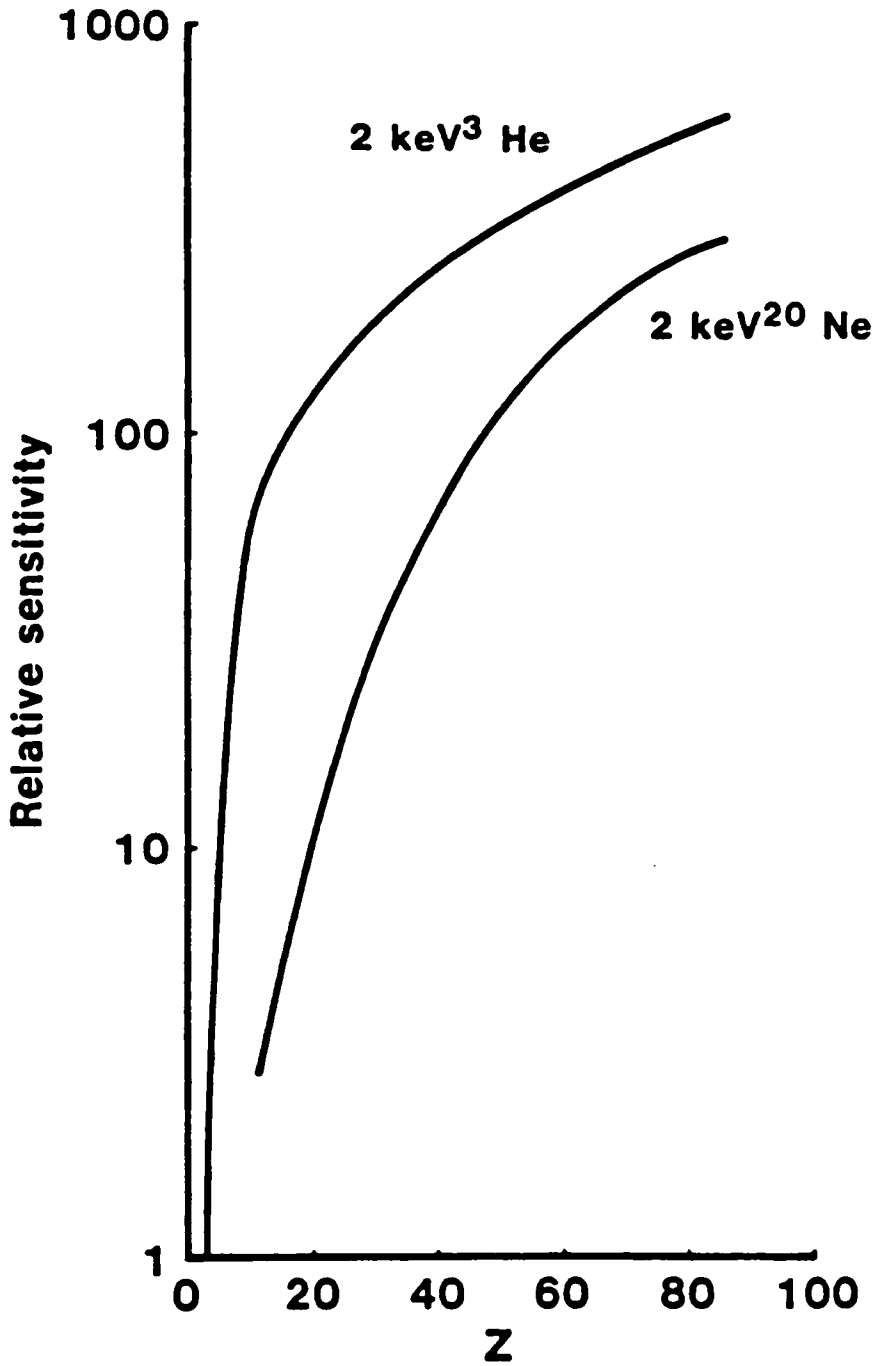

Figure 4.4. Relative elemental sensitivity vs. atomic number for ^{3}He and ^{20}Ne at 2 keV (104).

from the walls of the plasma chamber to the sample surface.

The ISS and XPS results are consistent in that an increasing amount of oxygen and a decreasing amount of fluorine was observed in both sets of spectra for samples exposed to an oxygen plasma for increasing time. Also a decrease in the amount of fluorine was found for composite samples which were gritblast, 5 minute argon plasma, and 7 minute argon plasma followed by 5 minute ammonia plasma pretreated, while a large amount of nitrogen present was found for samples which were 7 minute argon followed by 5 minute ammonia plasma pretreated.

C. PAS-FTIR

The purpose of the PAS-FTIR analysis was to complement the XPS and ISS surface analyses in identifying the elements present on the composite surfaces before and after pretreatment. The photoacoustic FTIR spectrum of a methanol washed composite sample is shown in Figure 4.5. This is the first reported PAS-FTIR spectrum of a carbon fiber/polyimide matrix composite. The assignments of the major peaks are given in Table 4.4. The peaks of 3071 and 2931 cm^{-1} are due to C-H stretching. The peaks at 1616 and 1518 cm^{-1} are attributed to C=C stretching of the substituted aromatic rings. Peaks associated with imide ring vibrations were observed and are consistent with the work of Dine-Hart and Wright (105). Asymmetric and symmetric carbonyl (C=0)

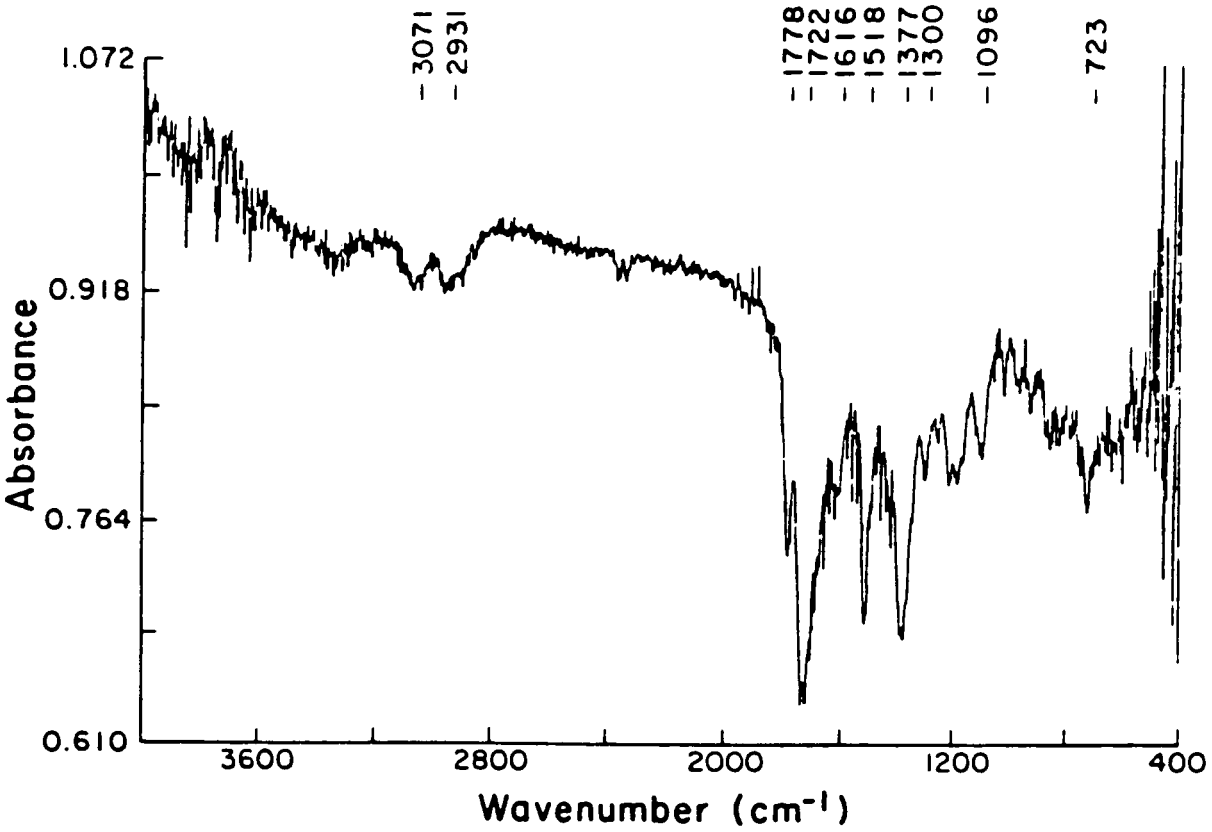

Figure 4.5. PAS-FTIR spectrum of a methanol washed LaRC-160/Celion 6000 carbon fiber composite.

TABLE 4.4

PAS-FTIR peak assignments for methanol washed composite.

Wavenumber	Assignment	
(cm-1)	Mode	Source
3071	C-H stretching	Aromatic
2931	C-H stretching	Aliphatic
1778	Asymmetric C=O stretching	Ester or imide ring
1722	Symmetric C=O stretching	Ester or imide ring
1616	C=C stretching	Aromatic ring
1518	C=C stretching	Substituted aromatic ring
1377	Axial vibration	C-N-C of imide ring
1300	Axial vibration	C-N-C of imide ring
1096	Transverse vibration	C-N-C of imide ring
723	Out of plane vibration	C-N-C of imide ring

stretching in the imide ring or from unreacted monomer (ester) are assigned to both the 1778 and 1722 cm^{-1} peaks. The peaks at 1377 and 1300 cm^{-1} are due to axial vibration of C-N-C of the imide ring. Transverse vibration of C-N-C of the imide ring is assigned to the 1096 cm^{-1} peak, whereas the out of plane vibration of C-N-C of the imide is attributed to the 723 cm^{-1} peak.

The PAS technique requires minimal sample preparation, that is, the sample needs only to be cut to fit the photoacoustic cell. Thus it is a convenient technique to establish group identification of solid surfaces. However, the analysis depth in PAS-FTIR is on the order of microns and therefore it is significantly greater than in either XPS or ISS (106). No differences in the PAS-FTIR spectra were noted for composite samples even after 20 minute exposure to an oxygen plasma in sharp contrast to the XPS and ISS results (see Table 4.1 and 4.3 respectively). Thus, the PAS-FTIR technique does not appear to be sensitive to changes in chemical composition in the topmost surface. These FTIR results are consistent with the conclusions of Cole, et al. (107) who used diffuse reflectance FTIR to study surface contamination of a graphite/epoxy composite. The authors concluded that 200 g/cm^2 (about 2000 nm) was the detection limit of contamination by this method. It is expected that the sampling depths of diffuse reflectance and photoacoustic will be similar for composites. It is not surprising then

that if plasma exposure produces change only in the topmost surface, the XPS and ISS results will readily reflect these changes, whereas the changes will remain undetected by PAS.

2. Wettability

Wettability can be very important in adhesion and can affect it in two ways. Incomplete wetting produces interfacial defects, lowering the adhesive bond strength. Secondly, better wetting can increase adhesive bond strength by increasing the work of adhesion which has been shown to be directly proportional to the fracture energy of a bond (68). The term wetting means that the contact angle between a liquid and a solid is zero or so close to zero that the liquid spreads over the solid easily. Non-wetting means that the angle is greater than 90^{o} so that the liquid tends to ball up and run off the surface easily (108).

The results in this section are aimed at understanding changes in the wettability of the composite surfaces before and after surface pretreatment. The effect of surface pretreatment on interfacial contact angle measurements is shown in Figures 4.6 and 4.7. The solvent diglyme was chosen because that was the solvent used to apply the LaRC-TPI as a primer to the pretreated composite adherends. Because the composite surfaces are not homogeneous and are not smooth, some scatter in the contact angle measurements was present. The large contact angle of 93 ± 14 for deionized water on the

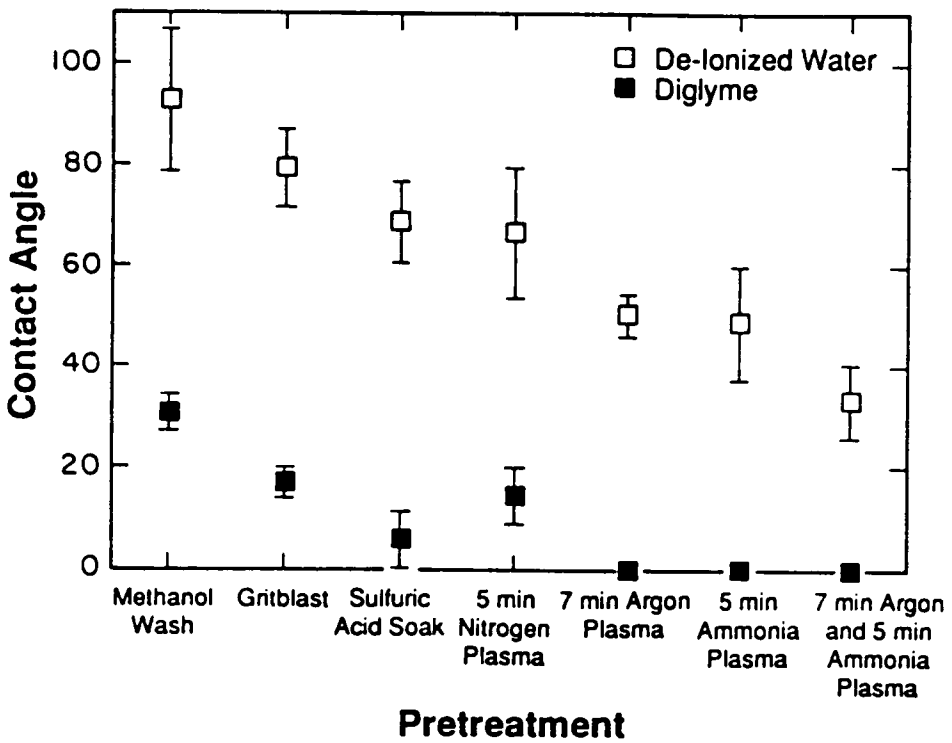

Figure 4.6. Effect of surface pretreatment on contact angle.

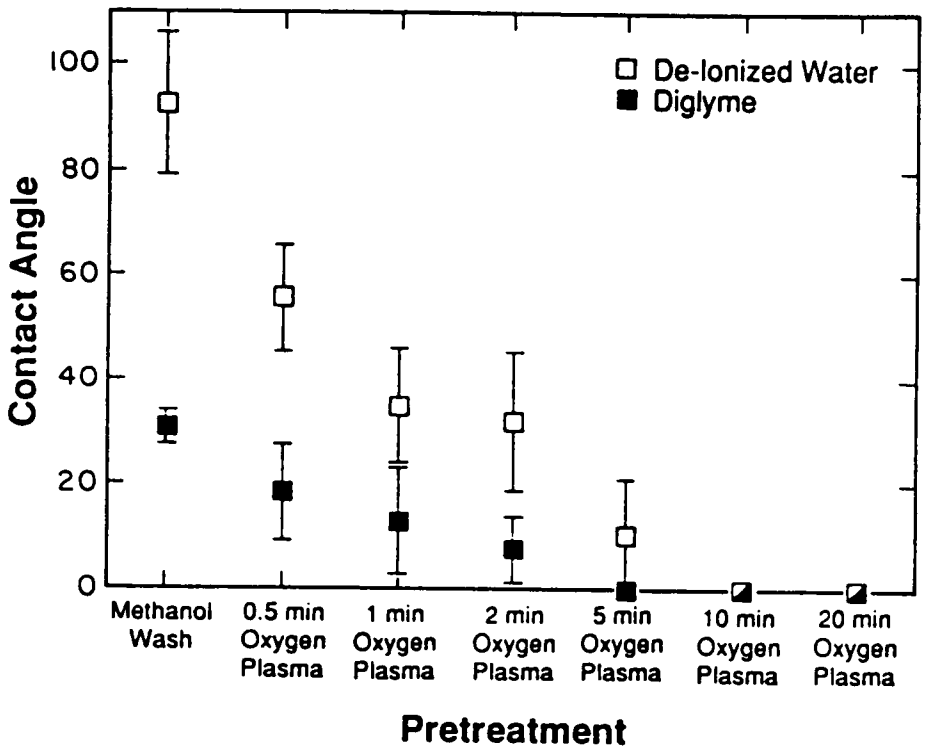

Figure 4.7. Effect of oxygen plasma pretreatment on contact angle.

methanol washed sample demonstrates that the methanol washed pretreated composite surfaces do not wet well. This result is not unexpected since the XPS data revealed that over 35 percent of the surface is a fluorocarbon. The reported water contact angle of polytetrafluoroethylene (PTFE) is 112^{o} (109). Reduction of the fluorocarbon on the surface, as in the case of the gritblasted composite surfaces, reduced the contact angle. In the case of the gritblast pretreated samples, reduction of the contact angle could also be attributed to increased roughening of the surface. The 5 minute nitrogen plasma and the 5 minute ammonia plasma composite surfaces demonstrate that the introduction of carbon-oxygen and carbon-nitrogen functionality, respectively, on the composite surfaces also reduces the observed contact angles. However, for both a decrease in the amount of fluorocarbon present on the surface along with an increase in surface functionality, an even larger reduction in the contact angle is produced. This increased wetting of the surface was observed for the 7 minute argon plasma, 7 minute argon plasma followed by 5 minute ammonia plasma and for all of the oxygen plasma pretreated surfaces. Complete wetting of the oxygen plasma surfaces occurred after 5 minutes. It can be clearly seen that the wettability of the pretreated composite surfaces increases due to a combination of a decrease in the amount of fluorocarbon and an increase in the carbon-oxygen and carbon-nitrogen functionality.

3. Topography

Surface pretreatment may affect the topography of composite surfaces. The results presented in this section are aimed at understanding changes in the topography of the composite surfaces before and after surface pretreatments. The surface topography of all of the composite pretreatments was studied by high resolution scanning electron microscopy, HR-SEM. Photomicrographs of the composite surfaces following the different surface treatments are shown in Figures 4.8-4.11. The methanol washed sample was used as a reference for comparison of the other surface pretreatments. For all surface pretreatments two distinct areas were observed, namely a smooth matrix region and secondly a region where fibers were observed. In Figure 4.8, these two regions can be seen for the methanol washed samples at 1600X magnification. Figure 4.8A is a photomicrograph of a smooth matrix region and Figure 4.8B is a photomicrograph of a region where fibers were observed. With the exception of the gritblast samples, all the pretreatments yielded surfaces which looked like the methanol washed composite, at 1600X magnification. The photomicrographs of the gritblast surfaces at 1600X magnification are shown in Figure 4.9. Gritblasting the composite surface produces a macroroughening of the surface affecting both the matrix and the fiber areas. Macroroughening is defined as roughening of the surface observed at low magnification (1600X) which is not observed

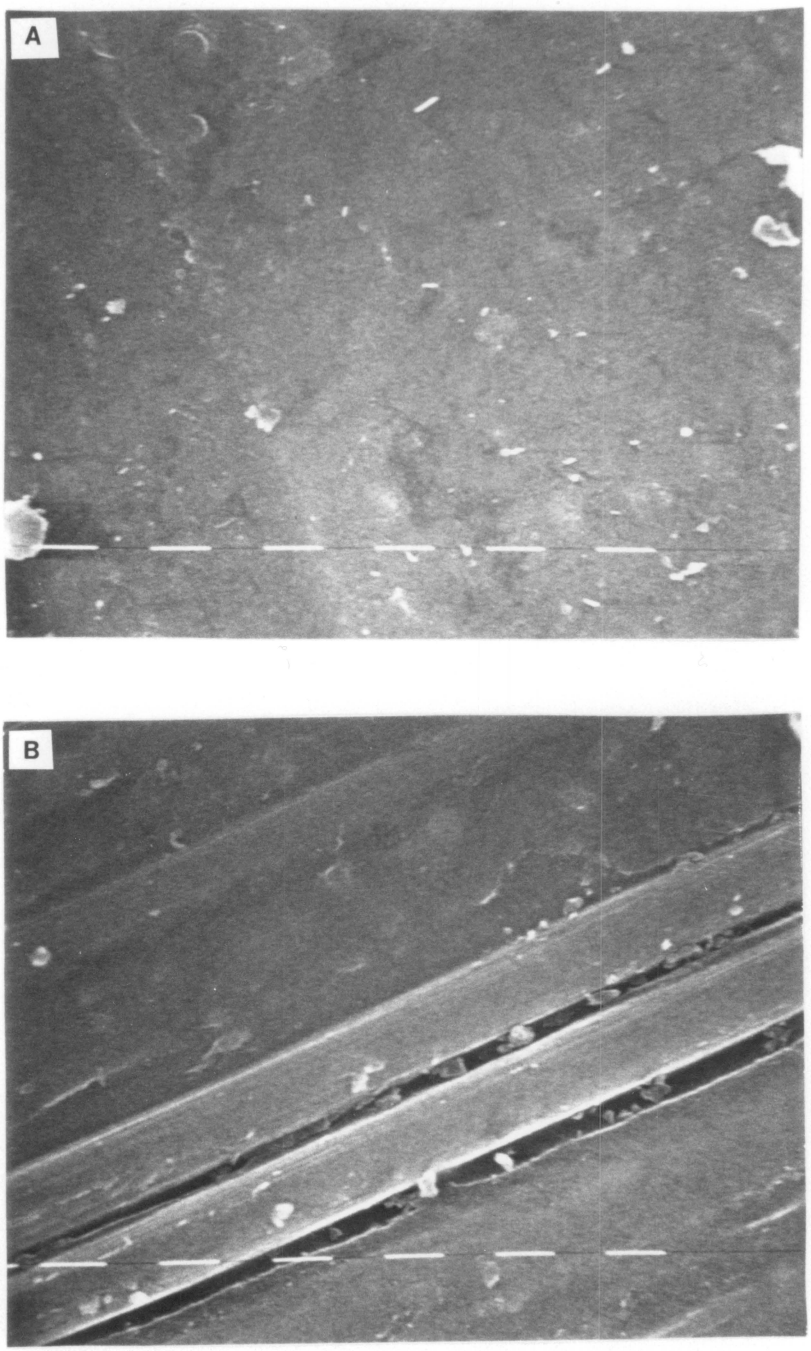

Figure 4.8. SEM photomicrographs at 1600X of methanol washed pretreated composites. Bar denotes 5 μm. (A) Matrix region (B) Fiber region.

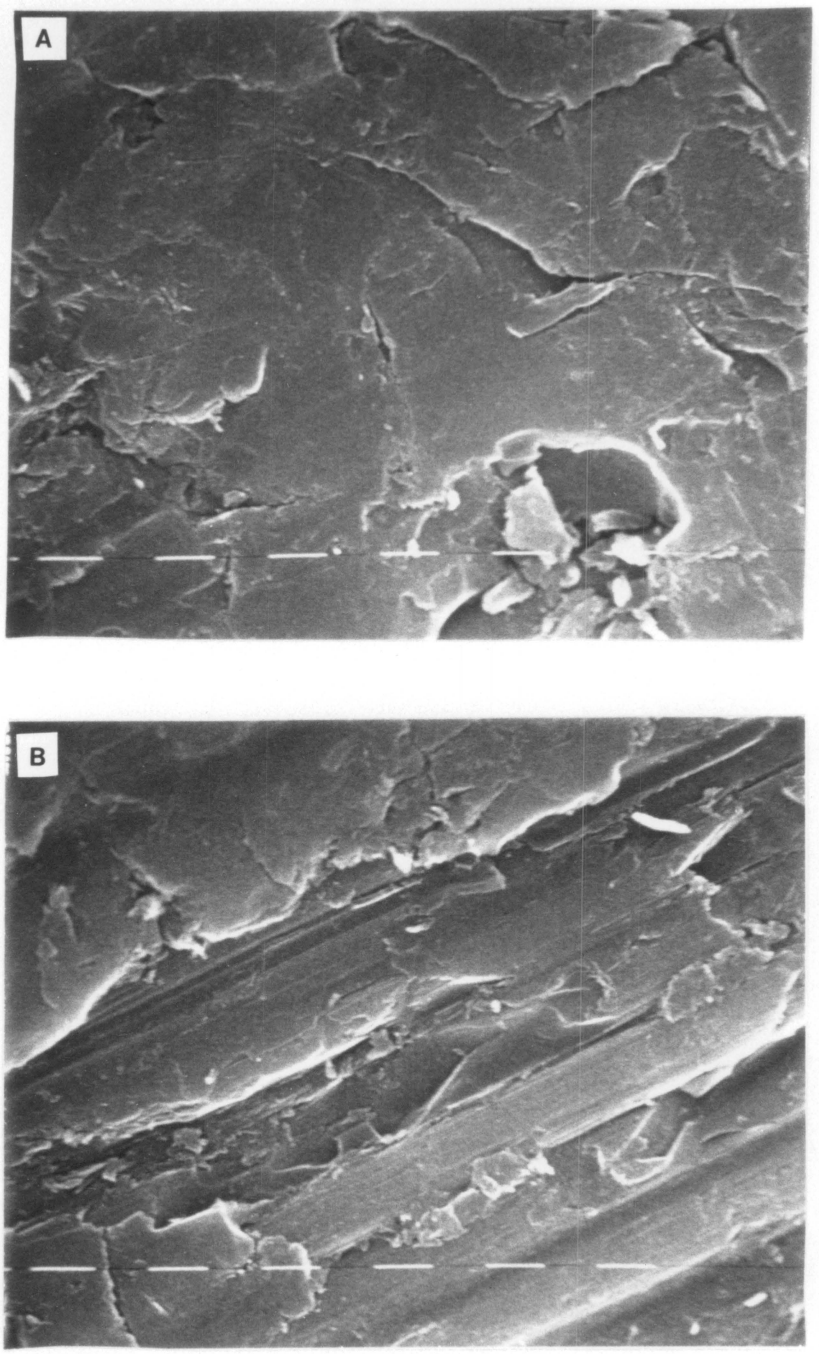

Figure 4.9. SEM photomicrographs at 1600X of gritblast pretreated composites. Bar denotes 5 μm. (A) Matrix region (B) Fiber region.

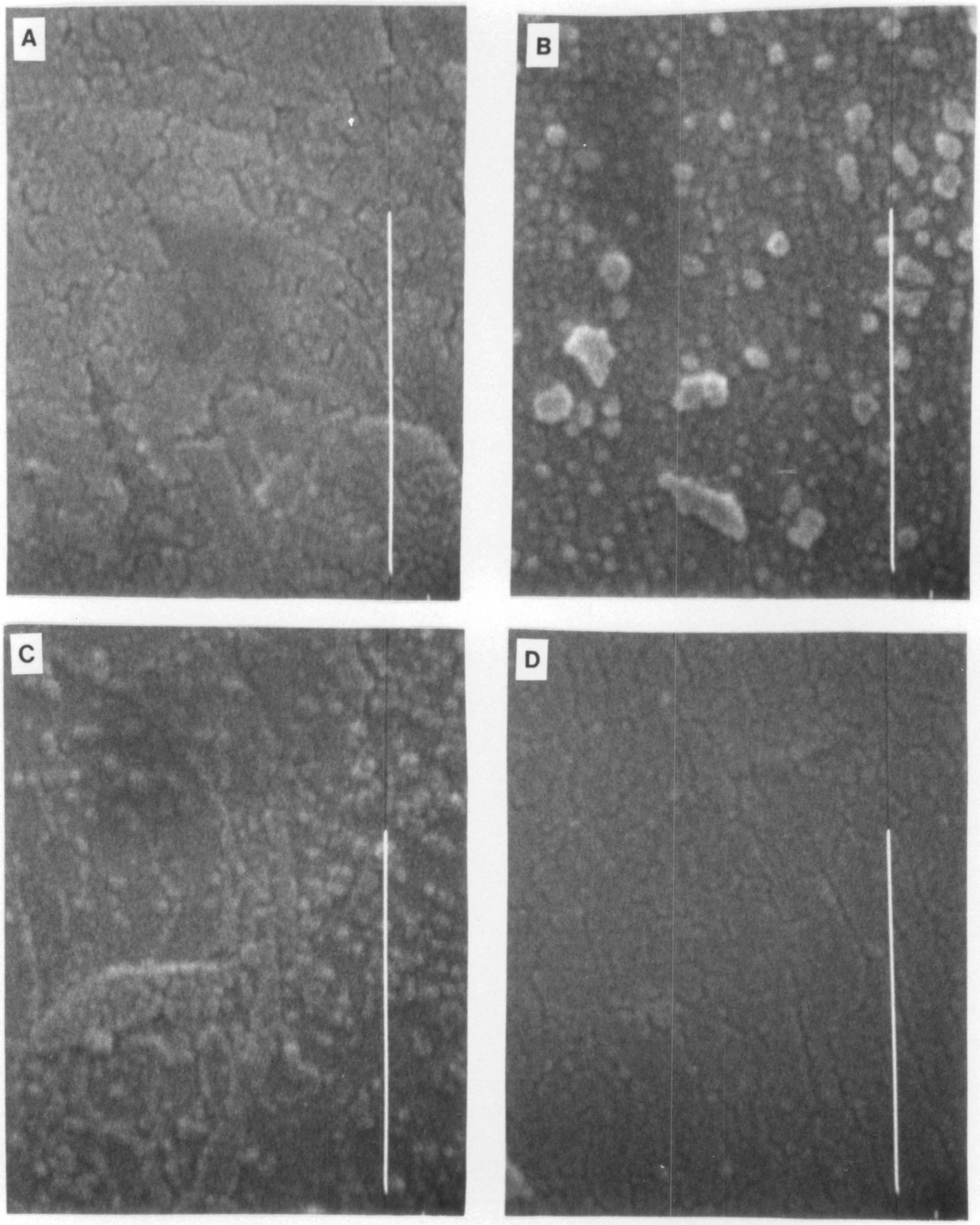

Figure 4.10. SEM photomicrographs at 100,000X of pretreated composites. Bar denotes 0.5 μm. (A) Methanol wash (B) 5 min. nitrogen plasma (C) 5 min. ammonia plasma (D) Gritblast (E) 5 min. oxygen plasma (F) 7 min. argon plasma followed by 5 min. ammonia plasma.

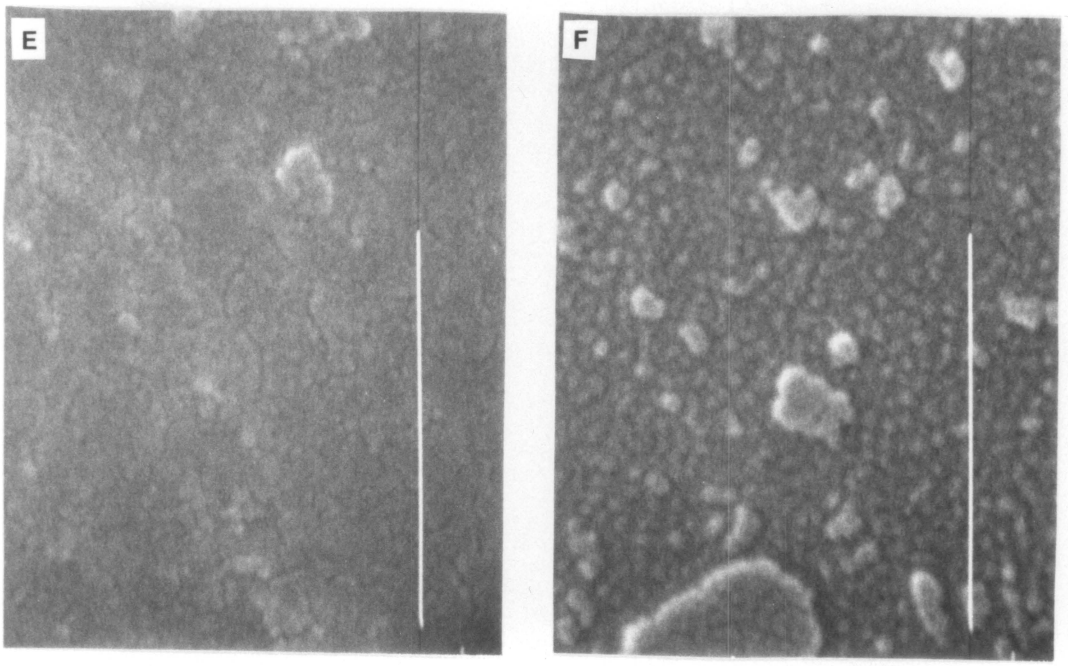

Figure 4.10. (continued).

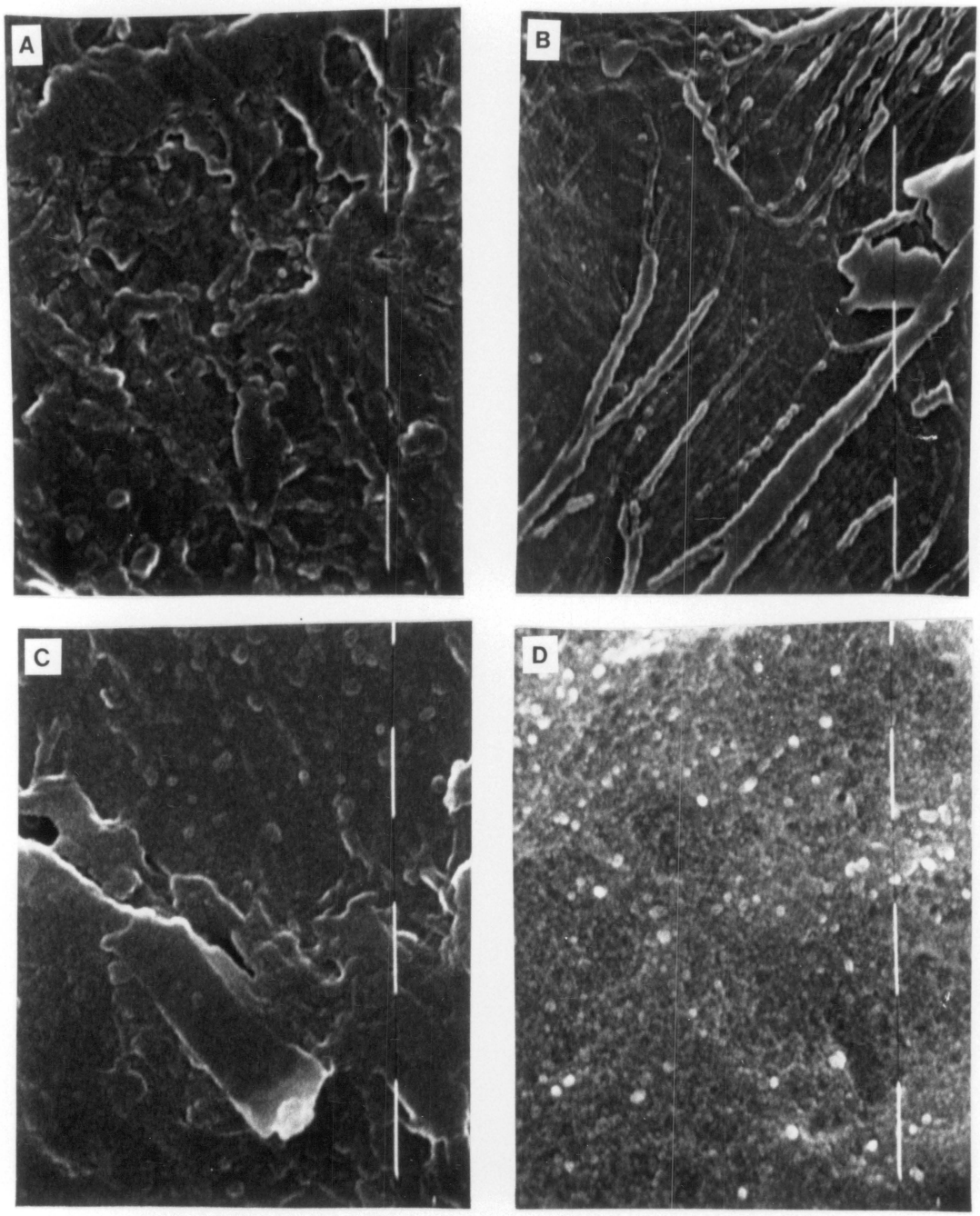

Figure 4.11. SEM photomicrographs at 25,000X of oxygen plasma pretreated composites. Bar denotes 0.5 μm. (A) 0.5 min. oxygen plasma (B) 1 min. oxygen plasma (C) 2 min. oxygen plasma (D) 5 min. oxygen (E) 10 min. oxygen plasma (F) 20 min. oxygen plasma.

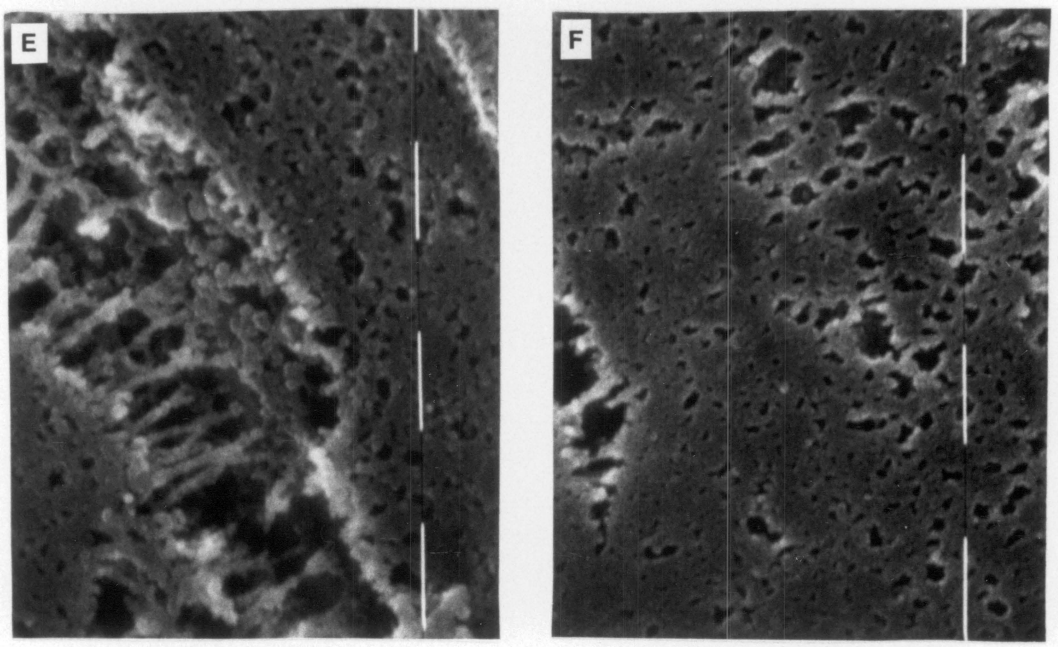

Figure 4.11. (continued).

at higher magnification (25,000X). This macroroughening of the surface could also damage the fibers which could reduce the strength of the composite. Figure 4.10 consists of photomicrographs of methanol washed, 5 minute nitrogen plasma, 5 minute ammonia plasma, gritblast, 5 minute oxygen plasma and 7 minute argon plasma followed by 5 minute ammonia plasma composite surfaces at 100,000X magnification. Although there are slight differences, the topography of all the surface pretreatments in Figure 4.10 appear to be similar. Figure 4.11 consists of photomicrographs of oxygen plasma treated surfaces at 25,000X magnification. The oxygen plasma appears to etch away and roughen the sample with pitting of the surface which is readily seen for 10 and 20 minute oxygen plasma treated samples.

The photomicrographs show the topography of the methanol washed, the 5 minute ammonia plasma, the 5 minute nitrogen plasma, the 7 minute argon plasma followed by 5 minute ammonia plasma, and the 5 minute oxygen plasma pretreated composite surfaces are comparably smooth which indicates that the adhesion was not influenced by surface roughening which could promote mechanical interlocking. However, the gritblast and the 10 and 20 minute oxygen plasma pretreated composite surfaces were roughened which could promote mechanical interlocking. Matienzo et al. attribute increased bond strengths of adhesively bonded composite materials to not only

decreased levels of contamination of the substrates but also to roughening of the composite surfaces (86).

B. Adhesive Bonding of Composites

Initially, the 16-ply panel made at the NASA-Langley Research Center was pretreated by either methanol washing, gritblasting or 0.5, 1, 2, 5 and 20 minutes oxygen plasma. This group of samples will be referred to as set one. The methanol wash pretreatment was chosen because it leaves the composite surface as close to the original after the removal of any contaminants which could occur due to handling. The gritblast procedure was chosen because it was shown in the previous results reported in Chapter IV, Section A.1.a. that the fluorocarbon contamination is reduced. Also solvent washing or wiping and gritblasting are the two most commonly used pretreatments used in industry today. The oxygen plasma pretreatment was chosen because it was shown in the previous results reported in Chapter IV, Section A.1.a. that oxygen plasma reduces the fluorocarbon contamination present on the composite surface, while also increasing the oxygen incorporated into the surface.

Secondly, the 14-ply panels made at Rockwell International were pretreated by either methanol washing, 5 minute nitrogen plasma, 5 minute oxygen plasma, 5 minute ammonia plasma or 7 minute argon plasma followed by 5 minute ammonia plasma. This group of samples will be referred to as

set two. The methanol wash pretreatment was chosen again because it yielded a composite surface as close to the original composite surface without contaminants due to handling. The 5 minute nitrogen plasma was chosen because previous results reported in Chapter IV, Section A.1.a. showed that this pretreatment increased the amount of oxygen incorporated into the surface while not reducing the fluorocarbon contamination present on the surface. The 5 minute oxygen plasma pretreatment was chosen again because previous results reported in Chapter IV, Section A.1.a. revealed that this pretreatment yielded a surface with only trace amounts of fluorocarbon contamination and an increase in the oxygen incorporated into the surface. Previous results reported in Chapter IV, Section A.1.a. showed that the 5 minute ammonia plasma pretreatment yielded composite surfaces with an increase in nitrogen functionality without a reduction in the fluorocarbon contamination present on the surface. The 7 minute argon plasma followed by the 5 minute ammonia plasma pretreatment was chosen because previous results reported in Chapter IV, Section A.1.a. revealed that a reduction in the fluorocarbon contamination and an increase in both oxygen and nitrogen incorporated into the composite surface were observed.

1. Wedge Test

a. Initial Crack Length

The effect of pretreatment on the average initial crack length with error bars of one standard deviation of adhesively bonded samples in set one which were methanol wash, gritblast or 0.5, 1, 2, 5, and 20 minute oxygen plasma pretreated is shown in Figure 4.12. Based on the results of the initial crack length, the oxygen plasma is the better pretreatment than the methanol wash and gritblast since the oxygen plasma yielded the smallest initial crack length. Although there is overlap in the error bars, one-way analysis of variance, the LSD and the Duncan's Multiple-Range Test were performed on the data and there are definite statistical differences between the mean crack lengths of the methanol washed and gritblasted samples as opposed to the 1, 2, 5 and 20 minute oxygen plasma pretreated composite samples.

The effect of pretreatment on the average initial crack length with error bars of one standard deviation of adhesively bonded wedge samples in set two which were methanol washed, 5 minute oxygen plasma, 5 minute ammonia plasma, 5 minute nitrogen plasma and 7 minute argon followed by 5 minute ammonia plasma pretreated is shown in Figure 4.13. Although one-way analysis of variance does not result in statistical differences among all of the pretreatments, the LSD and Duncan's Multiple-Range Test do show that the average initial crack length of the oxygen plasma pretreated surfaces is

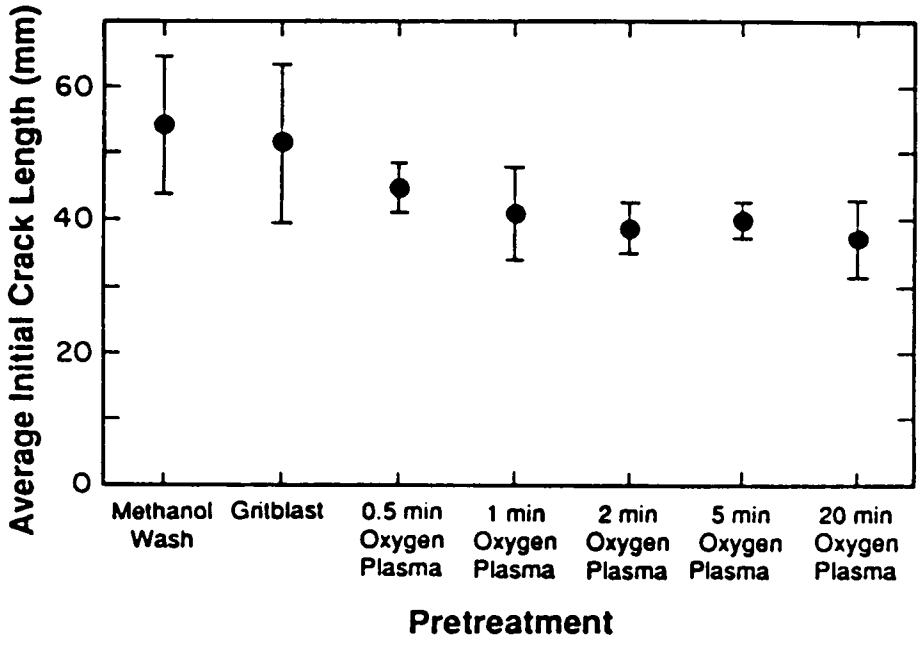

Figure 4.12. Effect of pretreatment on initial crack length with one standard deviation for wedge samples in set one.

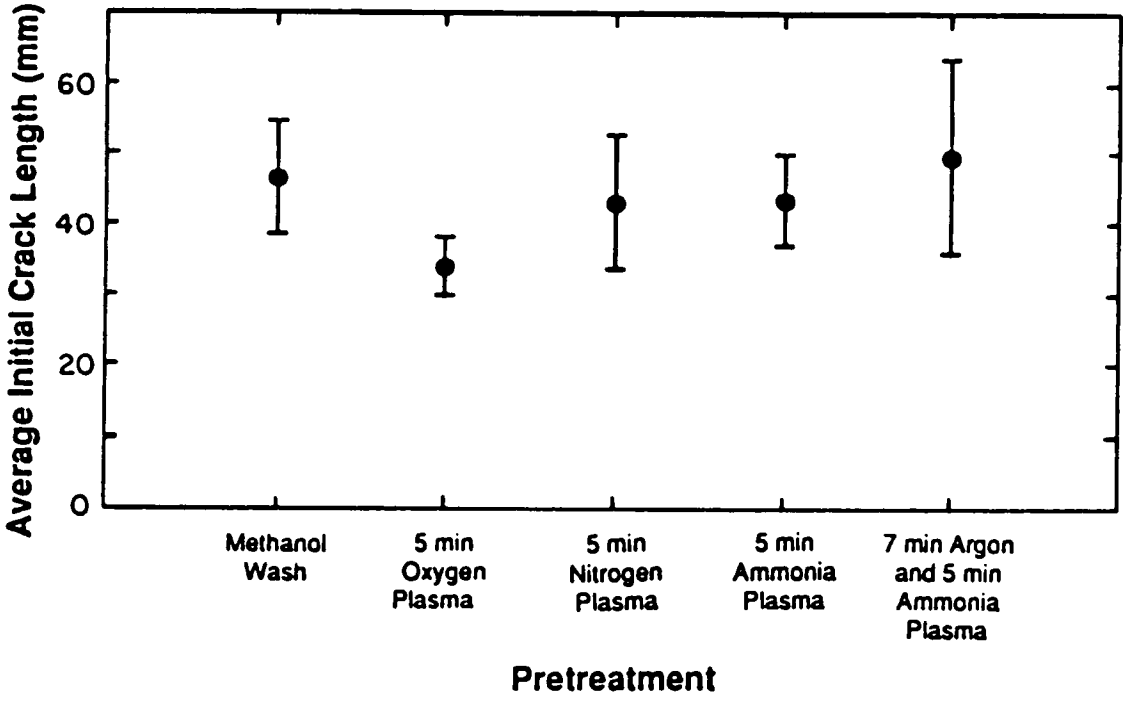

Figure 4.13. Effect of plasma pretreatment on initial crack length with one standard deviation for wedge samples in set two.

statistically different from the methanol washed and the argon plasma followed by the ammonia plasma pretreated surfaces. That is the oxygen plasma is the best pretreatment, since it yielded the smallest initial crack length, whereas the methanol wash and the argon followed by ammonia plasma pretreatments yielded the largest initial crack length and are the poorest pretreatments. These results are consistent with the results from set one wedge samples in that the oxygen plasma was the best surface pretreatment while the methanol wash was one of the poorest pretreatments. These results are also consistent with the work of Parker (85) who showed that the initial crack length was related to both the surface coverage of the contaminant and to the strength of lap joints prepared from similar composites.

b. Environmental Testing

Wedge samples were placed in one of three environments to determine the effect of surface pretreatment on crack propagation. The three environments chosen were (i) room temperature, desiccator for 1000 hours, (ii) 204^{o}C for 1000 hours and (iii) immersion in boiling water until failure.

Figures 4.14 and 4.15 show the average crack length with error bars of one standard deviation versus time for set one samples which have been methanol washed, gritblasted and 5 and 20 minute oxygen plasma pretreated and have been placed in a desiccator at room temperature for 1000 hours and in a 204^{o}C

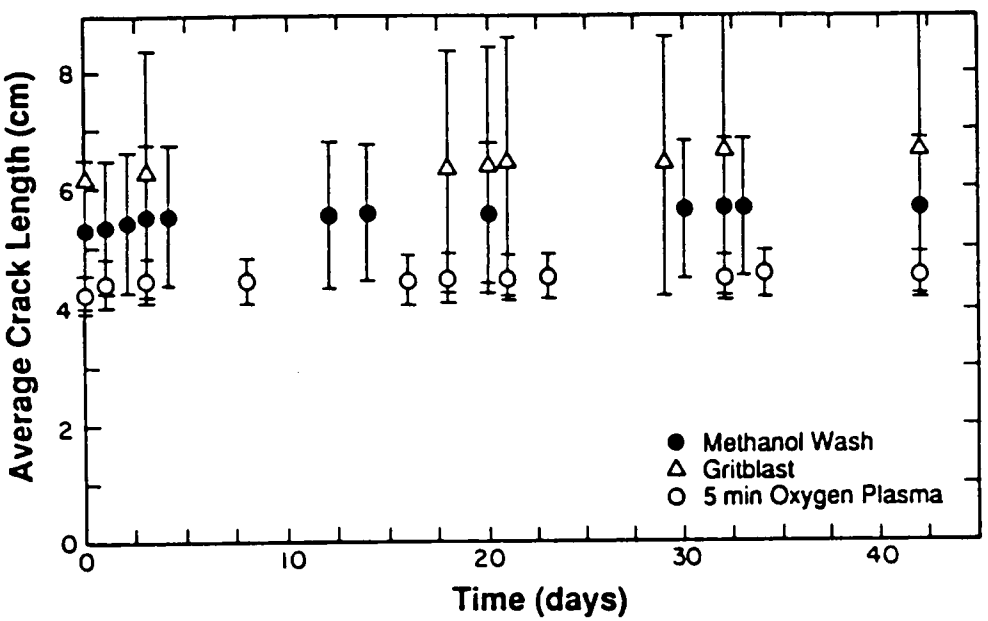

Figure 4.14. Effect of pretreatment on crack propagation with one standard deviation for set one wedge samples placed in a desiccator at room temperature for 1000 hours.

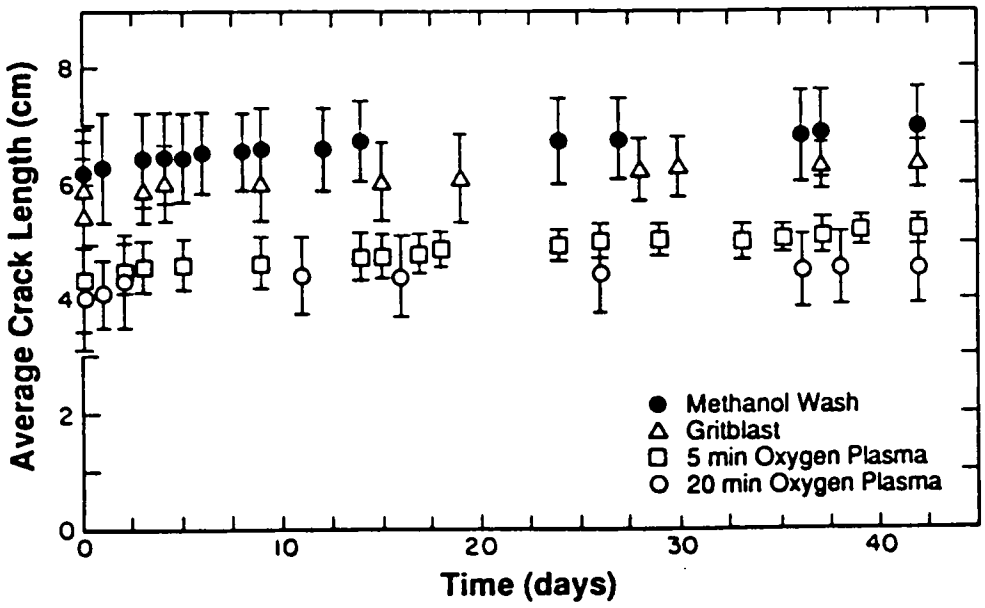

Figure 4.15. Effect of pretreatment on crack propagation with one standard deviation for set one wedge samples exposed to 204°C for 1000 hours.

oven for 1000 hours, respectively. Figure 4.16 shows the effect of pretreatment on the average time to failure with error bars of one standard deviation for methanol wash, gritblast and 5 minute oxygen plasma pretreated wedge samples in set one immersed in boiling water. A hot-wet environment is considered to be one of the harshest conditions for adhesively bonded joints. The paper in the appendix addresses the effect of a hot-wet environment on adhesively bonded Ti 6Al-4V wedge samples. Here, the critical strain energy release rate decreased as exposure time in hot water increased. Also failure became more interfacial as the wedge samples were exposed for longer times.

For room temperature and high temperature environments, the oxygen plasma yielded the shortest average crack length at any given time in comparison to the methanol washed and gritblasted samples. Even though there is some overlap in error bars, statistical analyses, specifically analysis of variance and multiple comparison tests, were employed. The analysis of variance results demonstrate that there are definite statistical differences between the average crack lengths for the pretreated surfaces. The LSD and Duncan's Multiple Range Test both showed that each surface pretreatment yielded results statistically different from all of the other surface pretreatments.

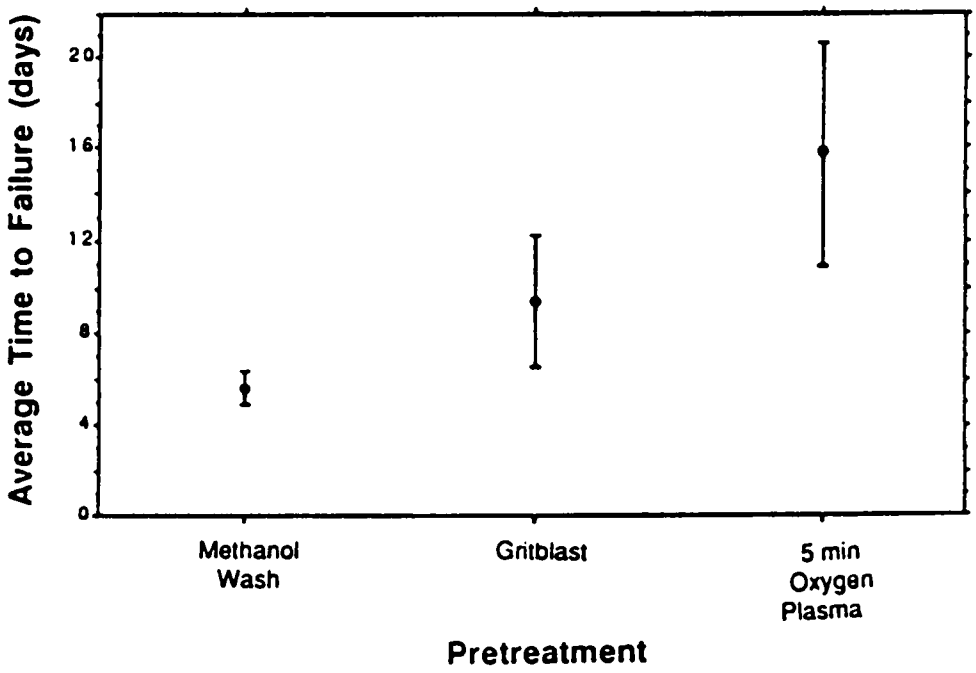

Figure 4.16. Effect of pretreatment on the average time to failure with one standard deviation for composite wedge samples in set one immersed in boiling water.

For adhesively bonded wedge samples immersed in boiling water, the 5 minute oxygen plasma yielded the longest average time to failure in comparison to the methanol washed and the gritblasted samples. Both the LSD and Duncan's Multiple Range Test showed that the 5 minute oxygen plasma pretreatment was statistically different than the methanol wash pretreatment.

Plots of average crack length versus time for set two wedge samples which have been methanol wash, 5 minute nitrogen plasma, 5 minute oxygen plasma, and 7 minute argon plasma followed by 5 minute ammonia plasma pretreated and then placed in a desiccator at room temperature for 1000 hours and in a 204^{o}C oven for 1000 hours are shown in Figures 4.17 and 4.18 respectively. The results of Figures 4.17 and 4.18 with error bars of one standard deviation are shown in Figures 4.19 and 4.20, respectively. Again, statistical analyses were performed on the data. The analysis of variance results indicate that definite statistical differences exist for the average crack lengths for all the pretreatments for both room temperature and high temperature environments. For the room temperature wedge testing, the LSD and Duncan's Multiple Range Test both showed the oxygen plasma to be the best pretreatment followed by nitrogen plasma. The argon plasma followed by the ammonia plasma was the worst pretreatment. No statistical differences exists between the methanol wash and the ammonia plasma pretreated samples. For the high temperature wedge testing, the LSD and Duncan's Multiple Range Test both showed

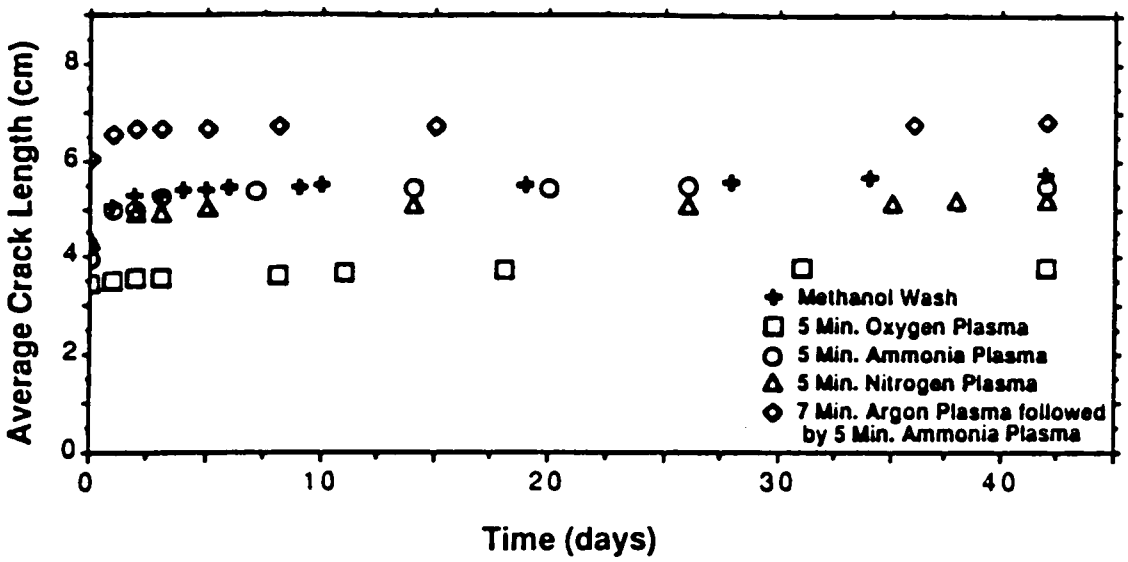

Figure 4.17. Effect of plasma pretreatment on crack propagation for set two wedge samples placed in a desiccator at room temperature for 1000 hours.

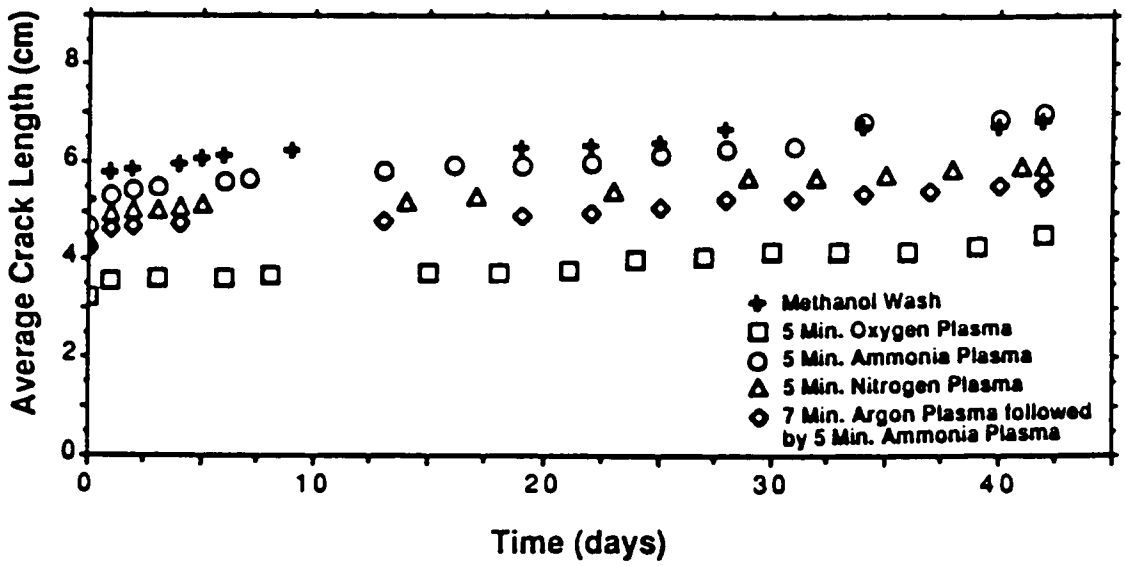

Figure 4.18. Effect of plasma pretreatment on crack propagation for set two wedge samples exposed to 204°C for 1000 hours.

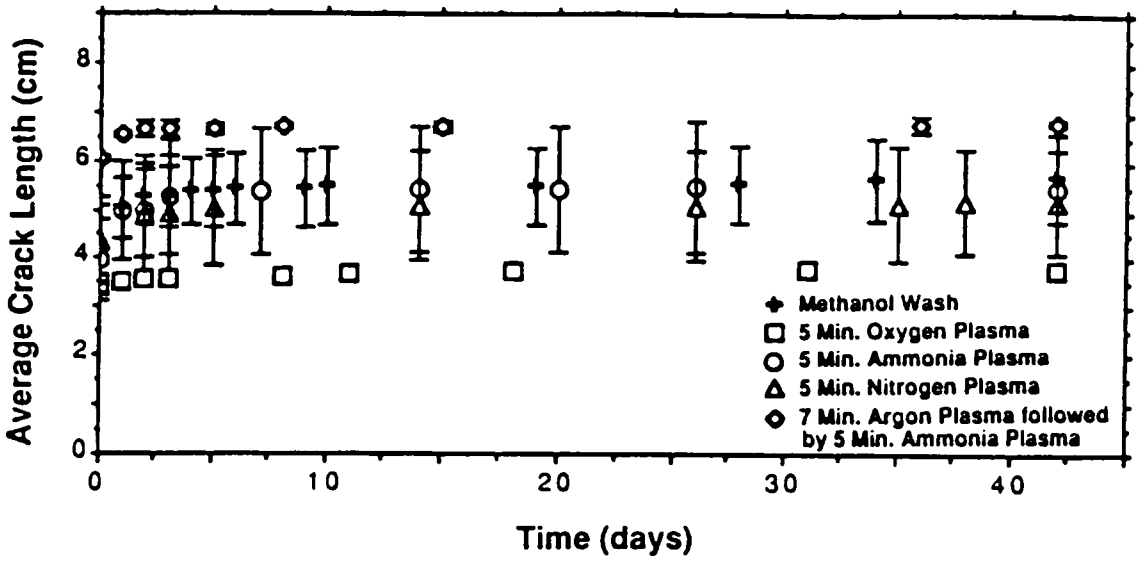

Figure 4.19. Effect of plasma pretreatment on crack propagation with one standard deviation for set two wedge samples placed in a desiccator at room temperature for 1000 hours.

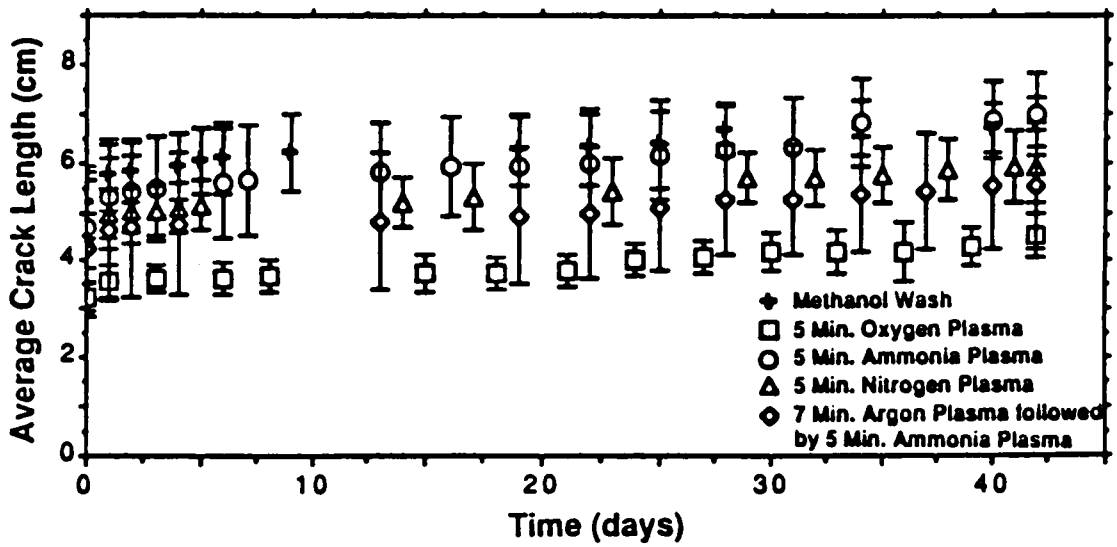

Figure 4.20. Effect of plasma pretreatment on crack propagation with one standard deviation for set two wedge samples exposed to 204°C for 1000 hours.

that each surface pretreatment yielded results statistically different from all the other surface pretreatments. Again the oxygen plasma pretreated samples yielded the smallest average crack length as a function of time and the methanol wash pretreatment yielded the largest average crack length as a function of time.

For all three environments and for both sets of wedge tests, the oxygen plasma pretreatment was always shown to be the pretreatment of choice. This improved bonding may be attributed to the fact that the oxygen plasma pretreatment both decreases the fluorocarbon contamination and increases the surface oxygen containing functionality. This increased surface functionality and decrease in fluorocarbon contamination causes better wetting of the adherend surface and the potential for covalent bonding at the primer-composite interface. In addition, the wedge test was shown to be sensitive to surface pretreatment. These are the first reported results which show that the wedge test is sensitive to surface pretreatment in various environments for adhesively bonded composites. This is in contrast to the work reported by Parker (85) which showed that crack growth was not a function of surface pretreatment, for epoxy bonded composite wedge samples exposed to a hot-humid environment.

c. Locus of Failure

When adhesively bonded composites debond, three different loci of failure may be observed. When failure occurs at the primer-composite adherend interface, interfacial failure is observed. Cohesive failure occurs when failure occurs within the adhesive itself, while composite failure occurs within the composite adherend. When adhesively bonded composites debond it is not unusual for more than one locus of failure to be observed. However, usually one predominant locus of failure exists.

The effect of pretreatment on the locus of failure for set one wedge samples which were methanol wash, gritblast and oxygen plasma pretreated is shown in Table 4.5. Figure 4.21 shows three debonded set one wedge samples, which were placed in a desiccator for 1000 hours at room temperature, and have been either methanol washed, gritblasted or 5 minute oxygen plasma pretreated. A different locus of failure is visually observed for each sample. However, after the wedge samples had debonded, the failed surfaces were also examined using XPS to determine the locus of failure. Fluorine was detected on both sides of failed methanol washed samples. Therefore the primary mode of failure for the methanol washed samples was interfacial between the primer and the composite adherend. Hence it is not surprising that the methanol washed samples gave larger crack lengths, and poorer durability than oxygen plasma treated samples.

TABLE 4.5

Effect of pretreatment on locus of failure for set one wedge samples.

	Environment		
Pretreatment	Room Temperature Desiccator 1000 Hours	204°C 1000 Hours	Boiling Water to Failure
Methanol Wash	Interfacial Cohesive	Interfacial	Interfacial Cohesive
Gritblast	Composite Interfacial	Composite	Composite Cohesive
Oxygen Plasma	Cohesive	Interfacial	Cohesive

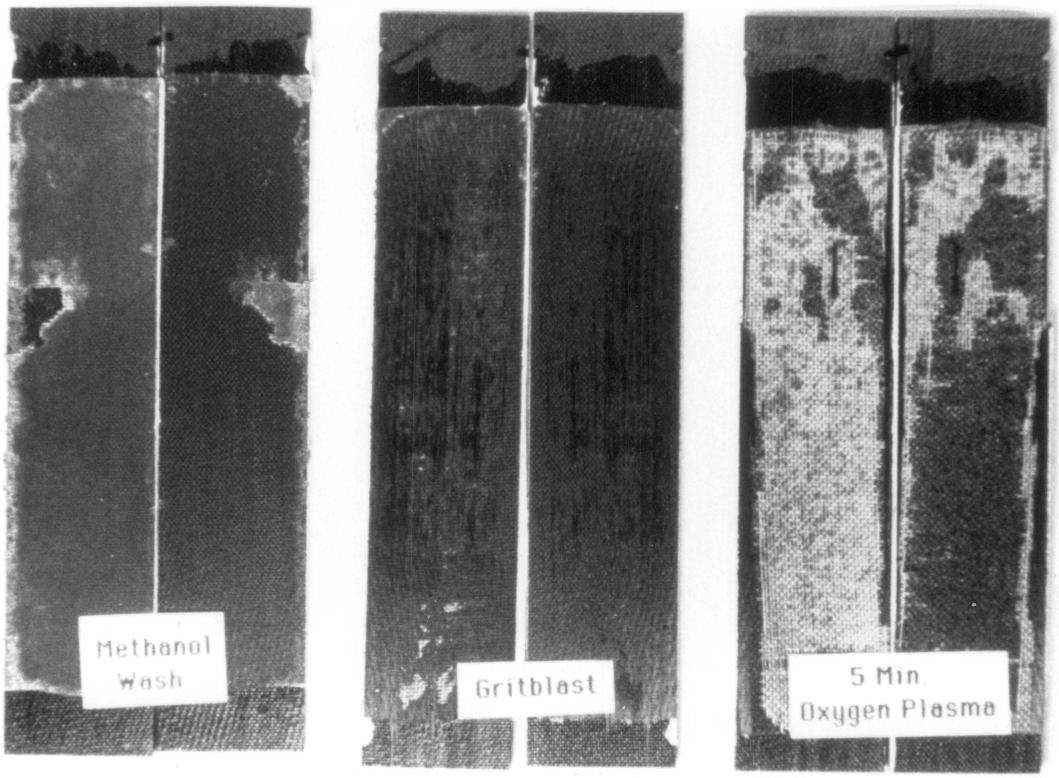

Figure 4.21. Debonded composite wedge samples which have been placed in a desiccator for 1000 hours at room temperature. (A) Methanol wash (B) Gritblast (C) 5 minute oxygen plasma.

The primary mode of failure for gritblast pretreated joints was interlaminar failure in the composite itself. Gritblasting is one of the most commonly used pretreatments for adhesively bonding composite joints today. However, these results of failure occurring within the composite confirm that even though gritblasting improves adhesion between the adhesive and the composite, gritblasting also produces flaws in the composite adherend itself forcing failure to occur within the weakened composite.

Cohesive failure was observed for oxygen plasma pretreated joints, except for the interfacial failure observed for the samples which were exposed to 204^{o}C for 1000 hours. Failure in the adhesive itself demonstrates that the oxygen plasma pretreatment provides good adhesion at the interface between the LaRC-TPI and the composite, while not weakening the composite adherend which occurs when gritblasting.

The effect of pretreatment on the locus of failure for set two wedge samples which were methanol wash, 5 minute nitrogen plasma, 5 minute oxygen plasma, 5 minute ammonia plasma and 7 minute argon plasma followed by 5 minute ammonia plasma pretreated is shown in Table 4.6. These results are consistent with those reported in Table 4.5, in that the methanol washed samples failed interfacially, while the oxygen plasma wedge samples failed cohesively.

Ammonia plasma, nitrogen plasma and argon plasma followed by ammonia plasma pretreated surfaces all failed

TABLE 4.6

Effect of plasma pretreatment on locus of failure for set two wedge samples.

Pretreatment	Room Temperature Desiccator 1000 hours	204°C 1000 hours
Methanol Wash	Interfacial	Interfacial
5 minute Nitrogen Plasma	Interfacial Cohesive	Interfacial
5 minute Oxygen Plasma	Cohesive	Interfacial Cohesive
5 minute Ammonia Plasma	Interfacial	Interfacial
7 minute Argon Plasma followed by 5 minute Ammonia Plasma	Interfacial	Interfacial

interfacially. These results show that in order for the best interfacial contact to exist between the primer and the composite adherends, reduction of fluorocarbon contamination to trace amounts and a large increase in the surface oxygen functionality are both necessary. As stated before, the reduction in the fluorocarbon contamination and the incorporation of functionality on the composite surface produce a surface which wets better and also a surface where potential covalent bonding can occur between the primer and the adherend surface.

2. Single Lap Shear Test

a. Single Lap Shear Strengths

Single lap shear joints were made from methanol wash, gritblast and 5 minute oxygen plasma pretreated composites. This group of samples will be referred to as set one. The average breaking strengths for single lap shear samples aged in a desiccator at room temperature for 1000 hours, for samples environmentally aged at 204^{o}C for 1000 hours, and for samples immersed in boiling water for three days are reported in Table 4.7. Statistical analyses, specifically one-way analysis of variance and the LSD and Duncan's multiple comparisons tests were employed on the lap shear test results. These results show that at room temperature and at high temperature, no difference in lap shear strengths were observed between pretreatments. Although no differences were

TABLE 4.7

Single lap shear strengths ± one standard deviation for bonded composite joints in set one after different surface pretreatments.

	Single Lap Shear Strengths (MPa)		
Pretreatment	Room Temperature Desiccator 1000 hours	204°C 1000 hours	Immersion in Boiling Water 3 days
Methanol Wash	18.8 ± 4.3	10.2 ± 2.3	12.2 ± 5.7
Gritblast	16.2 ± 2.1	11.5 ± 1.2	23.2 ± 2.4
5 min. Oxygen Plasma	23.5 ± 5.1	10.8 ± 3.4	24.9 ± 3.4

observed between pretreatments there was a reduction in the average lap shear strengths for samples which were environmentally aged at 204°C for 1000 hours as opposed to those which were placed in a desiccator for 1000 hours. However, in a hot-wet environment, such as immersion in boiling water, differences in lap shear strengths were observed for different pretreatments. The methanol washed samples gave lower lap shear strengths in comparison to the gritblast and oxygen plasma pretreated samples.

A second set of single lap shear joints were made from methanol wash, 5 minute nitrogen plasma, 5 minute oxygen plasma, 5 minute ammonia plasma and 7 minute argon plasma followed by 5 minute ammonia plasma pretreated composites. This group of samples will be referred to as set two. The average breaking strengths for set two single lap shear samples environmentally aged in a desiccator at room temperature for 1000 hours, for set two samples placed in 204°C for 1000 hours and for set two samples immersed in boiling water for three days are reported in Table 4.8. One-way analysis of variance and the LSD and Duncan's multiple comparisons tests were used to statistically analyze the lap shear strength results. One-way analysis of variance results reveal that at room temperature and at high temperature definite statistical differences do occur between average lap shear strengths of different pretreatments. Specifically, the LSD and Duncan's Multiple Range Test both showed that the

TABLE 4.8

Single lap shear strengths ± one standard deviation for bonded composite joints in set two after different plasma pretreatments.

	Single Lap Shear Strengths (MPa)		
Pretreatment	Room Temperature Desiccator 1000 hours	204°C 1000 hours	Immersion in Boiling Water 3 days
Methanol Wash	11.6 ± 1.3	10.5 ± 4.3	14.1 ± 2.5
5 min. Nitrogen Plasma	16.2 ± 2.5	9.2 ± 1.3	13.2 ± 7.5
5 min. Oxygen Plasma	22.2 ± 6.1	17.2 ± 1.7	18.9 ± 2.9
5 min. Ammonia Plasma	15.6 ± 1.7	10.0 ± 2.9	11.7 ± 6.7
7 min. Argon Plasma followed by 5 min. Ammonia Plasma	15.1 ± 1.4	8.4 ± 0.8	14.5 ± 5.6

oxygen plasma was statistically different from all of the other surface pretreatments for both the room temperature and high temperature environments. The oxygen plasma pretreated lap shear samples yielded the largest average breaking strength, making it the preferred pretreatment. In addition, a reduction in the average lap shear strengths for samples which were environmentally aged at 204°C for 1000 hours as opposed to those which were placed in a desiccator for 1000 hours was observed. However, for single lap shear samples immersed in boiling water statistical analysis show that no statistical differences exist between average breaking strengths for adhesively bonded composite samples with different adherend pretreatments.

Statistical differences were observed between pretreatments for all three environments, specifically immersion in boiling water for the first set of lap shear results discussed and room temperature and high temperature environments for the second set of lap shear results discussed. However, these results were not consistent for the results obtained from both sets of single lap shear samples evaluated in that statistical differences were not observed for the first set of lap shear samples exposed to room temperature and high temperature environments and for the second set of lap shear samples immersed in boiling water. Therefore, it can be concluded that the single lap shear test is able to distinguish between surface pretreatments for

adhesively bonded composite joints. In addition, with the exception of the first set of single lap shear samples environmentally aged at 204°C, the average single lap shear strength for all of the oxygen plasma pretreated samples was the largest making it the preferred pretreatment. This improved bonding may be attributed to the fact that the 5 minute oxygen plasma pretreatment decreases the fluorocarbon contamination to trace amounts and increases the surface containing functionality. This increased surface functionality and decrease in fluorocarbon contamination yields better wetting of the composite surface and the potential for covalent bonding at the composite-primer interface. These results are consistent with several studies which have shown that contamination of the composite surfaces by release agents can reduce the strength of lap shear joints (50,82-87). It has also been reported that chemical modification of composite surfaces by acid etching, plasma etching and corona-discharge pretreatments increase adhesive bond strengths by introducing specific functional groups on the surface (88-89).

b. Locus of Failure

Samples were examined after failure visually and through the use of XPS to determine the locus of failure. The effect of pretreatment on the locus of failure for set one single lap shear samples which have been methanol wash, gritblast and

oxygen plasma pretreated is shown in Table 4.9. Fluorine was detected on both sides of the debonded methanol washed samples which means that interfacial failure occurred. Gritblast samples failed within the composite. 5 minute oxygen plasma pretreated samples failed within the composite for samples kept at room temperature, interfacially for samples exposed to 204^{o}C and cohesively for samples which were immersed in boiling water.

The effect of pretreatment on the locus of failure for set two single lap shear samples which have been methanol wash, 5 minute nitrogen plasma, 5 minute oxygen plasma, 5 minute ammonia plasma and 7 minute argon plasma followed by 5 minute ammonia plasma pretreated is shown in Table 4.10. Again, fluorine was detected on both sides of the debonded methanol washed sample indicating interfacial failure. Interfacial failure was also observed for ammonia plasma pretreated composites. Both interfacial and composite failure was observed for samples which were nitrogen plasma and argon plasma followed by ammonia plasma pretreated. Composite failure was observed for samples which were oxygen plasma pretreated, indicating that good interfacial contact was achieved at the primer-adherend interface.

TABLE 4.9

Effect of pretreatment on locus of failure for single lap shear samples in set one.

	Environment		
Pretreatment	Room Temperature Desiccator 1000 Hours	204°C 1000 Hours	Boiling Water to Failure
Methanol Wash	Interfacial	Interfacial	Interfacial
Gritblast	Composite	Composite	Composite
5 Min. Oxygen Plasma	Composite	Interfacial	Cohesive

TABLE 4.10

Effect of pretreatment on locus of failure for plasma pretreated single lap shear samples in set two.

	Environment		
Pretreatment	Room Temperature Desiccator 1000 hours	204°C 1000 hours	Immersion in Boiling Water 3 days
Methanol Wash	Interfacial	Interfacial	Interfacial
5 min. Nitrogen Plasma	Interfacial Composite	Interfacial Composite	Interfacial Composite
5 min. Oxygen Plasma	Composite	Composite	Composite
5 min. Ammonia Plasma	Interfacial	Interfacial	Interfacial
7 min. Argon Plasma followed by 5 min. Ammonia Plasma	Interfacial Composite	Interfacial Composite	Interfacial Composite

V. SUMMARY

This work was conducted to observe the effect of surface pretreatment on the physical and chemical properties of carbon fiber-polyimide matrix composite surfaces and to understand how and why the differences in the pretreated composite surfaces are important to the bond strength and durability.

The eight pretreatments used, methanol wash, gritblast, sulfuric acid soak, ammonia plasma, argon plasma, argon plasma followed by ammonia plasma, nitrogen plasma and oxygen plasma, created surfaces with different properties. The results from both XPS and ISS showed a decrease in the amount of fluorine present for the gritblast, argon plasma, argon plasma followed by ammonia plasma, and oxygen plasma pretreated composite surfaces. Also there was an increase in the amount of oxygen incorporated into the surface for argon, argon followed by ammonia, nitrogen, and oxygen plasma pretreatments. The amount of oxygen incorporated into the oxygen plasma pretreated surface plateaued somewhere between 2 and 5 minutes. This increase in the atomic concentration of oxygen can be attributed to an increase in carbon-oxygen functionality. Finally, the XPS and ISS results showed an increase in the amount of nitrogen incorporated into the surface for ammonia and argon followed by ammonia plasma pretreated composites, which can be attributed to an increase in the amine functional groups already present on the

polyimide composite surface. The PAS-FTIR technique was not sensitive to changes in the topmost surfaces due to the sampling depth of PAS-FTIR.

The wettability of the pretreated composite surfaces increased as demonstrated with contact angle measurements, due to a combination of a decrease in the amount of fluorocarbon and an increase in the surface functionality present. No significant differences between the topography of the pretreated composites was observed, with the use of HR-SEM, with the exception of the macroroughening produced by gritblasting and the pitting produced by long exposure times (10 and 20 minutes) in the oxygen plasma.

Adhesive bond testing of these pretreated surfaces by the wedge test demonstrated that the initial crack length was sensitive to surface pretreatment. In addition, the wedge test was shown to be sensitive to surface pretreatment with the oxygen plasma yielding the smallest crack lengths and the most durable bonds when compared to all other pretreatments in a room temperature, high temperature and hot-wet environment. The single lap shear test was able to distinguish between surface pretreatments for composite samples environmentally aged at room temperature, at high temperatures and by immersion in boiling water. As with the wedge test results, the oxygen plasma pretreatment was the best pretreatment since the oxygen plasma surface pretreated single lap shear samples produced the largest lap shear

strengths. The superior adhesive bonding of the oxygen plasma in contrast to all of the other surface pretreatments may be attributed to a decrease in fluorocarbon contamination to trace amounts and an increase in oxygen surface functionality. This increased surface functionality and decrease in fluorocarbon contamination causes better wetting of the composite surface and may also lead to covalent bonding at the composite-primer interface.

In addition these results obtained address the three-fold objective stated in the INTRODUCTION section. First the results of the characterization of the pretreated composite surfaces coupled with the bonding studies demonstrated that surface pretreatment of the composite adherend is an important factor which affects both the strength and durability of adhesively-bonded composite materials. Therefore, in order to obtain the full potential of composite structures the surface pretreatment of the composite adherend must be optimized. Secondly, the results of the single lap shear test showed a reduction in the average lap shear strength for samples which were environmentally aged at high temperature as opposed to those environmentally aged at room temperature. Therefore, the single lap shear test can be used to evaluate new high temperature adhesives. Finally, changes in the pretreated composite surfaces, shown by the results of the physical and chemical characterization of the pretreated composite surfaces, combined with the differences observed in

the single lap shear and wedge test results, due to different surface pretreatments, demonstrated that changes in the composite adherend-primer interface or interphase have an important role in determining the performance of adhesively bonded composite joints.

VI. REFERENCES

1. J.R. Vinson, in Emerging Technologies in Aerospace Structures, Design, Structural Dynamics and Materials, J.R. Vinson, ed. The American Society of Mechanical Engineers, New York, 67 (1980).

2. J.E. Castle and J.F. Watts, in Interfaces in Polymer, Ceramic and Metal Matrix Composites, H. Ishida, ed., Elsevier Science Publishing Co., Inc., New York, 57 (1988).

3. L.T. Drzal, The Role of the Polymer-Substrate Interphase in Structural Adhesion, AFML-TR-77-129 (1977).

4. M.M. Schwartz, Composite Materials Handbook, McGraw-Hill Book Co., New York, 1984.

5. D.V. Rosato, in Handbook of Composites, G. Lulin, ed., Van Nostrand Reinhold Co., New York, 1982.

6. F.P. Gerstle, in Encyclopedia of Physical Science and Engineering, John Wiley and Sons, New York, 1985.

7. J.B. Donnet and R.C. Bansal, Carbon Fibers, Marcel Dekker, Inc., New York, 1984.

8. R.J. Diefendorf, W.C. Stevens, and S.H. Chen, Fiber Producer, 16, Dec. (1979).

9. R.J. Diefendorf, and E. Tokarsky, Polym. Eng. and Sci., 15, 150 (1975).

10. M. Oberlin and A. Oberlin, Rev. Chim. Miner., 18, 442 (1981).

11. R.L. Gordon, in Encyclopedia of Materials Science and Engineering, M.B. Bever, ed., the MIT Press, Mass., 1988.

12. J. Schultz, L. Lavielle and C. Martin, J. Adhesion, 23, 45 (1987).

13. L.T. Drzal, M.J. Rich and P.F. Lloyd, J. Adhesion, 16, 1 (1982).

14. L. Penn, F. Bystry, W. Karp and S. Lee, in Molecular Characterization of Composite Interfaces, H. Ishida and G. Kumar ed., Plenum, New York, (1985).

15. J.V. Mullin and V.F. Mazzio, J. Mech. Phys. Solids, 20, 391 (1972).

16. M.J. Owen, in Encyclopedia of Polymer Science and Engineering, M.B. Bever, ed., The MIT Press, Mass., 1988.

17. D.M. Brewis, in Industrial Adhesion Problems, D.M. Brewis and D. Briggs, ed., Orbital Press, Oxford, 1985.

18. American Society for Testing and Materials (ASTM), ASTM D 907-82 Standard Definitions of Terms Relating to Adhesives, 1982, published in volume 15.06 (Adhesives), 1984 Annual Book of ASTM Standards.

19. K.P. Subrahmanian, in Structural Adhesives; Chemistry and Technology, S.R. Hartshorn, ed., Plenum Press, New York, 1986.

20. A.K. St. Clair and T.L. St. Clair, "The Development of Aerospace Polyimide Adhesives," NASA Technical Memorandum 84587, January 1983.

21. A.H. Landrock, Adhesives Technology Handbook, Noyes Publications, New Jersey, 1985.

22. J. Shields, Adhesives Handbook, 2nd Edition, Newnes-Butterworth, London, 1976.

23. H.A. Burgman, J.H. Freeman, L.W. Frost, G.M. Bower, E.J. Traynor and C.R. Ruffing, J. Appl. Polym. Sci., 12, 805 (1968).

24. A.K. St. Clair and T.L. St. Clair, SAMPE Quarterly, 13(1), 20 (1981).

25. A.K. St. Clair, T.L. St. Clair, W.P. Bane and K.R. Bakshi, Proc. of the Printed Circuit World Exposition, 3 (1981).

26. V.L. Bell, U.S. Patent 4,094,862 to NASA-Langley Research Center, 1978.

27. T.L. St. Clair and R.A. Jewell, Proc. Eighth National SAMPE Tech. Conf., Washington, October (1976).

28. A.K. St. Clair, "Polyimides: Thermally Stable Aerospace Polymers" NASA Technical Memorandum 81884, October (1980).

29. E.M. Boroff and W.C. Wake, Trans. Inst. Rubber Industry, 25, 199 (1949).

30. D.E. Packam in Aspects of Adhesion 7, D.J. Alner and K.W. Allen, ed., Transcript Books, London, 1973.

31. D. Tabor and R.H.S. Winterton, Proc. Roy. Soc., A312, 435 (1969).

32. S.S. Voyutskii, in Autohesion and Adhesion of High Polymers, V. Vakula, ed., Interscience, New York, 1963.

33. B.V. Derjaguin, Research, 8, 70 (1955).

34. H. Krupp, J. Adhesion, 4, 83 (1972).

35. H. Krupp, J. Adhesion, 5, 269 (1973).

36. W.C. Wake, in Recent Advances in Adhesion, L.H. Lee ed., Gordon and Breach, New York, 1973.

37. M. Gettings and A.J. Kinloch, J. Material Sci., 12, 2511 (1977).

38. M. Gettings and A.J. Kinloch, Surface Interf. Analysis, 1, 189 (1980).

39. J.R. Huntsberger, Adhesives Age, 13, 43 (1970).

40. G.P. Anderson, S.J. Bennett and K.L. DeVries, Analysis and Testing of Adhesive Bonds, Academic Press, New York, 1977.

41. D. Broek, Elementary Engineering Fracture Mechanics, Sijthoff and Noordhoff International Publishers, New York, 1978.

42. ASTM Designation: D 1002, 1987.

43. L.J. Hart-Smith, Adhes. Age, 28, April, 1987.

44. D. Zalucha, in High Performance Adhesive Bonding, Garry De Frayne, ed., Society of Manufacturing Engineers, Michigan, 1983.

45. D. Volkersen, Luftfahrtforsch, 15, 412 (1938).

46. J.A. Marceau, Y. Moji and J.C. McMillian, Adhes. Age, 28, October, 1977.

47. G.P. Anderson, in Encyclopedia of Physical Science and Technology, R.A. Meyers, ed., Academic Press, New York, 1987.

48. A.C. Kennedy, R. Kohler and P. Poole, Int. J. Adhes. Adhes., 3(2), 133 (1983).

49. P. Commercon and J.P. Wightman, J. Adhesion, 22, 13 (1987).

50. T.A. DeVilbiss, D.L. Messick, D.J. Progar and J.P. Wightman, Composites, 16(3), 207 (1985).

51. J.A. Filbey, J.P. Wightman, and D.J. Progar, J. Adhesion, 20, 283 (1987).

52. C.U. Ko and J.P. Wightman, J. Adhesion, 24, 93 (1987).

53. J.J. Bickerman, Appl. Chem., 11, 81 (1961).

54. F.K. McTaggart, Plasma Chemistry in Electrical Discharges, Elsevier, Amsterdam, 1967.

55. H. Yasuda, H.C. Marsh, E.S. Brandt and C.N. Reilley, J. Polym. Sci., Polym. Chem. Ed., 15, 991 (1977).

56. D.T. Clark and A. Dilks, in Characterization of Metal and Polymer Surfaces, Vol. 2, L.H. Lee, ed., Academic Press, New York, 1977.

57. D.T. Clark and W.J. Weast, J. Macromol. Sci., C12(2), 191 (1975).

58. R.H. Hansen and H. Schonhorn, J. Polym. Sci., B4, 203 (1966).

59. R.R. Sowell, N.J. DeLollis, H.J. Gregory and O. Montoya, J. Adhes., 4, 15 (1972).

60. K. Rossmann, J. Polym. Sci., 19, 141 (1956).

61. M. Stradal and D.A.I. Goring, Can. J. Chem. Eng., 53, 427 (1975).

62. C.Y. Kim, J.M. Evans, D.A.I. Goring, J. Appl. Polym. Sci., 15, 1365 (1971).

63. D.K. Owens, J. Appl. Polym. Sci., 19, 265 (1975).

64. J.R. Hollahan, B.B. Stafford, R.D. Falb and S.T. Payne, J. Appl. Polym. Sci., 13, 807 (1969).

65. E.L. Lawton, J. Appl. Polym. Sci., 18, 1557 (1974).

66. A. Bradley and T.R. Heagney, Anal. Chem., 42, 894 (1970).

67. J.R. Hall, C.A.L. Westerdahl, M.J. Bodnar and D.W. Levi, J. Appl. Polym. Sci., 16, 1465 (1972).

68. S. Wu, Polymer Interface and Adhesion, p. 360, Marcel Dekker, Inc., New York, 1982.

69. N. Saka, G.Y. Yee, and N.P. Suh, 35th ANTEC, SPE, 337 (1977).

70. C.Y. Kim, G. Suranyi and D.A.I. Goring, J. Appl. Polym. Sci., C30, 533 (1970).

71. R.M. Lerner, Adhes. Age, 12(12), 35 (1969).

72. J. Osterndorf, R. Rosty and M.J. Bodnar, SAMPE J., 25(4), 15, July/August (1989).

73. H. Gleich, R.M. Criens, H.G. Mosle, and U. Lente, Int. J. Adhesion and Adhesives, 9, 88 (1989).

74. B. Westerlind, A. Larsson and M. Rigdahl, Int. J. Adhesion and Adhesives, 7, 141 (1987).

75. C.A.L. Westerdhahl, J.R. Hall, E.C. Schramn and D.W. Levi, J. Colloid Interface Sci., 47, 610 (1974).

76. N.J. DeLollis, Rubber Chem. Technol., 46, 549 (1973).

77. H.E. Wechsberg and J.B. Webber, Mod. Plast., 38(5), 199 (1961).

78. N.J. DeLollis and O. Montoya, J. Adhes., 3, 57 (1971).

79. H. Schonhorn, F.W. Ryan and R.H. Hansen, J. Adhes., 2, 93 (1970).

80. A. Baszkin and L. Ter-Minassian-Saraga, Polymer, 19, 1083 (1978).

81. L.W. Crane, C.L. Hamermesh, and L. Maus, SAMPE J., 6, March/April (1976).

82. D.K. Brewis, J. Comyn and J.R. Fowler, Polymer, 18, 76 (1977).

83. M.H. Stone, Int. J. Adhesion and Adhesives, 271, July (1981).

84. B.M. Parker and R.M. Waghorne, Composites, 13, 280, July (1982).

85. B.M. Parker, "An Evaluation of the Boeing Wedge Test for the Assessment of CFRP Surface Pretreatment" Royal Aircraft Establishment Tech. Memo MAT/STR 1038, March 1984.

86. L.J. Matienzo, J.D. Venables, J.D. Fudge and J.J. Velten, 30th National SAMPE Symp., 302, March 19-21, 1985.

87. B.M. Parker, "Adhesive Bonding of Contaminated Fibre Composites," in International Conference on Structural Adhesives in Engineering, Waveney Print Services, Suffolk, England, 123 (1986).

88. S.Y. Wu, A.M. Schuler and D.V. Keane, 19th Intern. SAMPE Tech. Conf., 277, October 13-15, 1987.

89. G.K.A. Kodokian and A.J. Kinloch, J. Mat. Sci. Letters, 7, 625 (1988).

90. T.A. DeVilbiss, D.J. Progar, and J.P. Wightman, Composites, 19, 67 (1988).

91. D.J. Progar, J. Adhesion Sci. Technol., 2, 449 (1988).

92. D. D'Agosta, March Instruments, private communication.

93. J.H. Scofield, J. Elect. Spect. and Rel. Phen., 8, 129 (1976).

94. M. Lentner, Introduction to Applied Statistics, Prindle, Weber and Schmidt, Boston, 1975.

95. W.H. Beyer, ed. CRC Handbook of Tables for Probability and Statistics, 2nd ed., CRC Press, Florida, 1968.

96. R.G.D. Steel and J.H. Torrie, Principles and Procedures of Statistics, 2nd ed., McGraw-Hill Book Co., New York, 1980.

97. J.C. Miller and R.N. Miller, Statistics for Analytical Chemistry, John Wiley and Sons, New York, 1984.

98. D.G. Madeleine, S.A. Spillane and L.T. Taylor, J. Vac. Sci. Technology, 5, 347 (1987).

99. G. Koranyi and T.M. Acs, Acta Chim. Hung., 24, 3337 (1960).

100. D.L. Messick, D.J. Progar, and J.P. Wightman, Surface Analysis of Graphite Reinforced Polyimide Composites, NASA Technical Memorandum 85700, October (1983).

101. D.S. Everhart and C.N. Reilley, Anal. Chem., 53, 665 (1981).

102. D. Briggs and C.R. Kendall, Int. J. Adhesion and Adhesives, 2, 13 (1982).

103. D.K. Mohanty, S.D. Wu and J.E. McGrath, Polymer Preprints, 29, 352 (1988).

104. A.C. Miller, "Low-energy Ion Scattering Spectroscopy" Alcoa Technical Paper, Alcoa Center, Pennsylvania, February 2, 1983.

105. R.A. Dine-Hart and W.W. Wright, Makromol. Chem., 143, 189 (1971).

106. C.Q. Yang, R.R. Bresee and W.G. Fateley, Appl. Spect. 41(5), 889 (1987).

107. K.C. Cole, L. Lehto and M. Yahasz, SPIE: Optical Techniques for Industrial Inspection, 665, 243 (1986).

108. A.W. Adamson, Physical Chemistry of Surfaces, 4th ed. John Wiley and Sons, New York, 1982.

109. J.R. Dann, J. Colloid Interface Sci., 32, 302 (1970).

Appendix Durability of Structural Adhesive Bonds in a Hostile Environment[1]

1. Abstract

Two surface chemistry aspects of the bonding of Ti 6Al-4V alloy with FM-300U epoxy adhesive were studied. First, X-ray photoelectron spectroscopy (XPS) was used to follow surface contamination of pretreated Ti 6Al-4V adherends prior to adhesive bonding. Second, moisture intrusion into adhesively bonded Ti 6Al-4V wedge samples was monitored by quantitative image analysis, calculation of critical strain energy release rates, (G_{Ic}) and by XPS. Failure became more interfacial and the critical strain energy release rates decreased as the samples were exposed to longer periods of immersion in water. The results suggest non-Fickian diffusion of water into the bondline.

2. Introduction

The durability of structural adhesive bonds in hostile environments is an area of continuing research (1-3). The main advantage in using adhesives for structural applications is the high strength to weight ratio of the bonded components. There is also an increase in design flexibility. However with

---

[1] Published in part in "Proceedings of Fifth International Joint Military/Government-Industry Symposium on Structural Adhesive Bonding at U.S. Army Armament Research and Development, and Engineering Center," Dover, New Jersey, November 3-5, 1987, and co-authored with J.P. Wightman, H.F. Brinson, D.A. Dillard and T.C. Ward.

the use of structural adhesives, a severe limitation commonly observed is the detrimental effect of moisture on the bond strength (4). Some studies have dealt with the behavior of water in cured epoxy resin from the viewpoint of water absorption and diffusion. The behavior of water at the interface in an adhesive bond has not yet been clarified quantitatively (5). The loss of bond strength and the mechanisms involved in environmental failure of structural adhesive joints are not well understood. The work presented in this appendix was done to quantify the effect of a contaminating environment on the surface composition of pretreated Ti 6Al-4V adherends and to study moisture intrusion into an epoxy/Ti 6Al-4V wedge sample.

3. Experimental

a. Materials

The Ti 6Al-4V alloy used was supplied by RMI Titanium. The FM-300U, a 175°C cure rubber-modified structural epoxy unscrimmed film adhesive, was supplied by American Cyanamid.

b. Contamination Study

Coupons of Ti 6Al-4V alloy were pretreated using a phosphate-fluoride etch (6). The samples were placed immediately after pretreatment in a Perkin-Elmer 5300 XPS spectrometer. After obtaining the initial survey spectrum and narrow scans on any significant peaks observed in the survey

scan spectra, the sample was cleaned in situ using an argon ion beam. A second set of spectra were obtained on the cleaned sample. The sample was then removed from the spectrometer and exposed to air for a specified period of time. The same sample was reinserted in the spectrometer and a third set of spectra were obtained followed by ion bombardment. This process was repeated several times. XPS angle studies (90^{o}, 30^{o} and 10^{o}) were also performed.

c. Moisture Intrusion

Wedge coupons, 2.54 x 15.24 x 0.38 cm were phospate-fluoride pretreated and bonded with two layers of FM-300U cut to the same dimensions as the wedge coupons leaving 1 cm. clear at each end. The thickness of the bondline was controlled using Teflon film spacers yielding a bondline thickness of 0.0381 cm. The wedge joints were placed in a platen press and heated from room temperature to 175^{o}C at 1.72 MPa bonding pressure for 1.5 hour. The heat was turned off and the joints allowed to cool to room temperature under pressure.

Moisture intrusion into Ti 6Al-4V wedge samples was studied by placing the wedge samples in deionized water at 98^{o}C for varying times. The samples were removed from the water. One set of samples were opened by a wedge driven manually into the samples and quantitative image analysis was used to determine the percentage of area of the failed

surfaces covered by adhesive. The other set of samples had a precrack of about 6 cm made in the bondline. The critical load (P_c) to propagate the crack was determined using an Instron model 1123. Values of G_{Ic}, the critical strain energy release rate, were calculated using the equation

$$G_{Ic} = 12\ P_c^2 a^2 / B^2\ Eh^3$$

where a is the length of the precrack [6 cm], B is the adherend width [2.54 cm], E is the modulus of the adherend [1.14 x 10^{11} Pascals] and h is the adherend thickness [0.38 cm]. The failure surfaces were analyzed by quantitative image analysis and by XPS.

4. Results and Discussion

a. Contamination Study

It is well known that pretreated solid surfaces contaminate readily upon exposure to laboratory conditions. However, the type, extent, and speed of contamination is not often documented (7) particularly in adhesion studies. Ti 6Al-4V samples were pretreated with a phosphate-fluoride etch and then exposed to the lab atmosphere for varying amounts of time. Careful attention was paid to the reference binding energy of the carbon 1s photopeak in order to give an unambiguous assignment of the bonding state of carbon on the pretreated surface. The results are summarized in Table A-1.

TABLE A-1

XPS analysis of phosphate-fluoride etched Ti 6Al-4V.

Time Interval	Take-Off Angle	Atomic Fraction C/Ti	Atomic Fraction O/Ti	Atomic Fraction Ar Sputtered C/Ti	Atomic Fraction Ar Sputtered O/Ti
30 sec	90°	1.5	4.1	0.68	4.1
60 sec	90°	1.2	4.0	0.59	3.8
150 sec	90°	1.3	4.1	0.68	3.8
300 sec	90°	1.2	4.2	0.47	3.9
13 hrs	90°	1.3	3.4		
13 hrs	30°	1.8	3.5		
13 hrs	10°	3.3	3.9		

The atomic fraction ratios of carbon to titanium and oxygen to titanium show that no significant differences were observed for samples exposed to the air for the various time periods ranging from 30 to 300 seconds. Angle studies for the sample which was exposed to the air for 13 hours showed that at a 10^{o} take-off angle, the carbon to titanium ratio more than doubled when compared to the 90^{o} take-off angle. Therefore, contamination is rapid and is limited to the topmost surface of the pretreated Ti 6Al-4V adherend. Argon sputtering of the samples reduced the carbon to titanium ratio and increased the oxygen to titanium ratio. Therefore sputtering with argon removed the carbon contamination present. This contamination may be attributed to adsorption of organic vapors from the lab environment.

b. Moisture Intrusion

The initial study was concerned with the quantitative image analysis of wedge samples opened after varying periods of exposure in hot water. Sketches of the visual appearance of the failure surfaces after different exposure times are shown in Figure A-1. The percentage of adhesive area on the failure surface is plotted as a function of exposure time in Figure A-2. It is assumed that diffusion of water into the bondline produces delamination. A linear decrease is noted in Figure A-2 consistent with non-Fickian diffusion of water into the bondline.

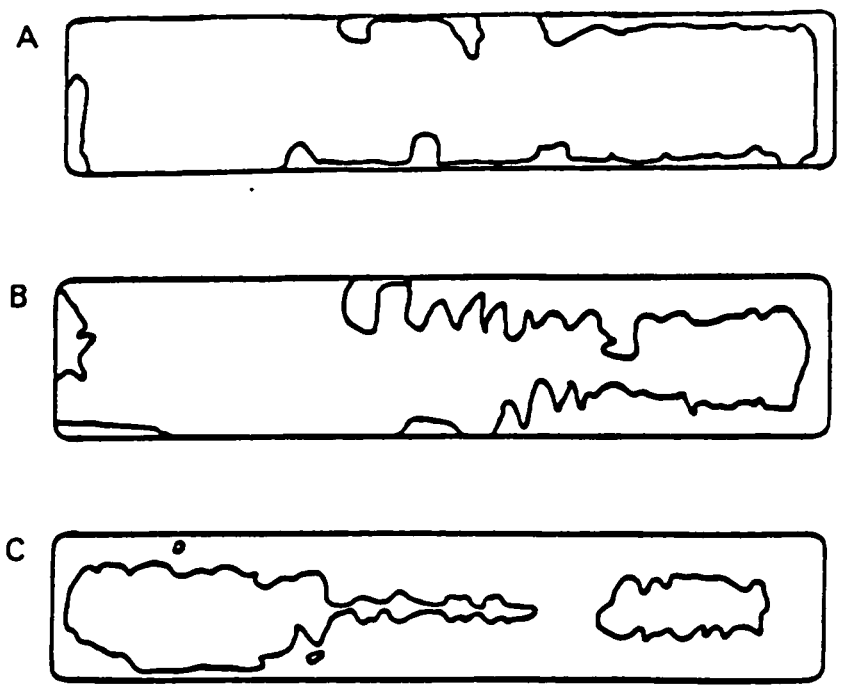

Figure A-1. Sketches of failure surfaces after opening phosphate-fluoride Ti 6Al-4V bonded with FM-300U wedge samples environmentally aged in 98°C water. (A) 1 day (B) 7 days (C) 14 days.

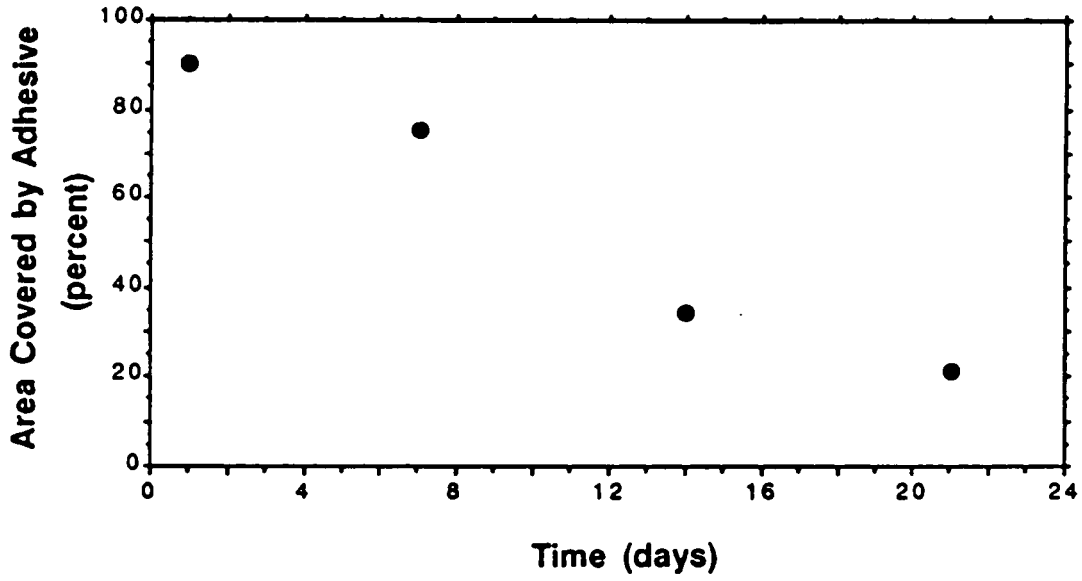

Figure A-2. Percent area of the adherend covered by adhesive vs. time phosphate-fluoride Ti 6Al-4V wedge samples bonded with FM-300U were immersed in 98°C water.

The critical strain energy release rate was determined in a more extensive study. Values of G_{Ic} are plotted against exposure time in Figure A-3. Again, a linear decrease was observed consistent with the results seen in Figure A-2. The zero day sample is taken as the control.

The failure surfaces in the more extended study were also analyzed by XPS and the results are shown in Table A-2. The C/Ti ratio decreased with increasing exposure times indicating decreasing amounts of residual adhesive left on the failure surface. Nitrogen is a tag element contained in the epoxy and the N/Ti ratio parallels the trend seen for the C/Ti ratio. The interpretation of changes in the oxygen photopeak for the four failure surfaces shown in Figure A-4 supports the decreasing amount of residual epoxy adhesive with increasing exposure time. A doublet is clearly seen for the 7 day sample. The higher binding energy peak at about 533 eV is associated with oxygen in the epoxy and is seen to decrease in intensity with increasing exposure time. Conversely, the lower binding energy peak at about 531 eV associated with oxygen in the surface oxide on the Ti 6Al-4V adherend is seen to increase in intensity with increasing exposure time.

5. Summary

The contamination of pretreated Ti 6Al-4V adherend surfaces is rapid and is due to partially reversible, multilayer adsorption of organic vapors from the lab

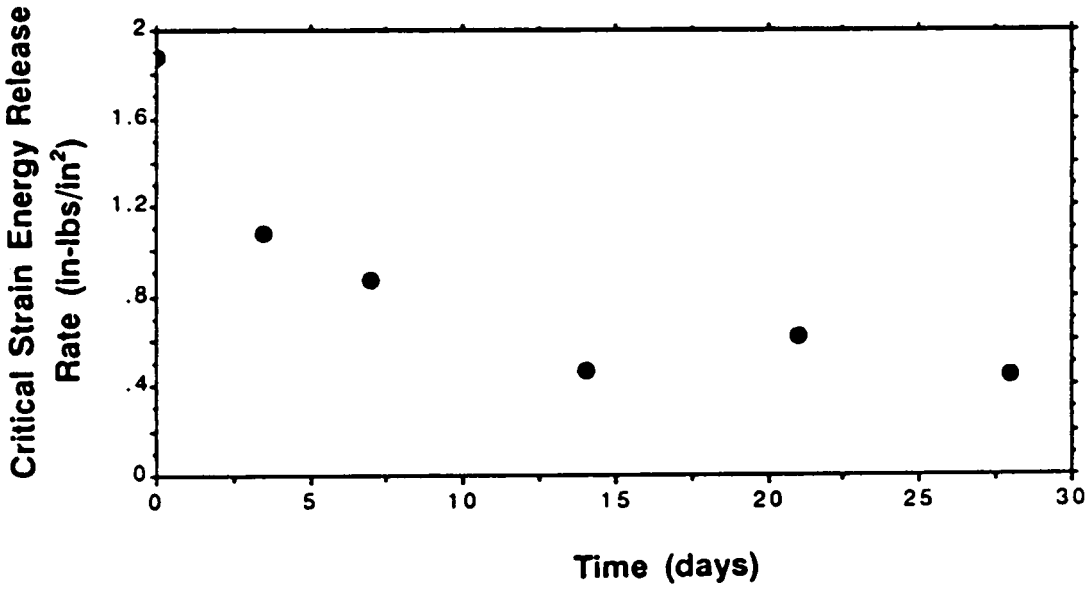

Figure A-3. Critical strain energy release rate vs. time Ti 6Al-4V wedge samples bonded with FM-300U were immersed in 98°C water.

TABLE A-2

XPS analysis of failure surfaces of phosphate-fluoride Ti 6Al-4V bonded with FM-300U wedge samples.

Time Immersed ($98^{o}C$ H_2O)	Visual Appearance	C/Ti	N/Ti
0 days	Adhesive	190	1.6
7 days	Film	13	0.47
28 days	Metal	6.4	0.18
P/F only	Metal	1.3	0

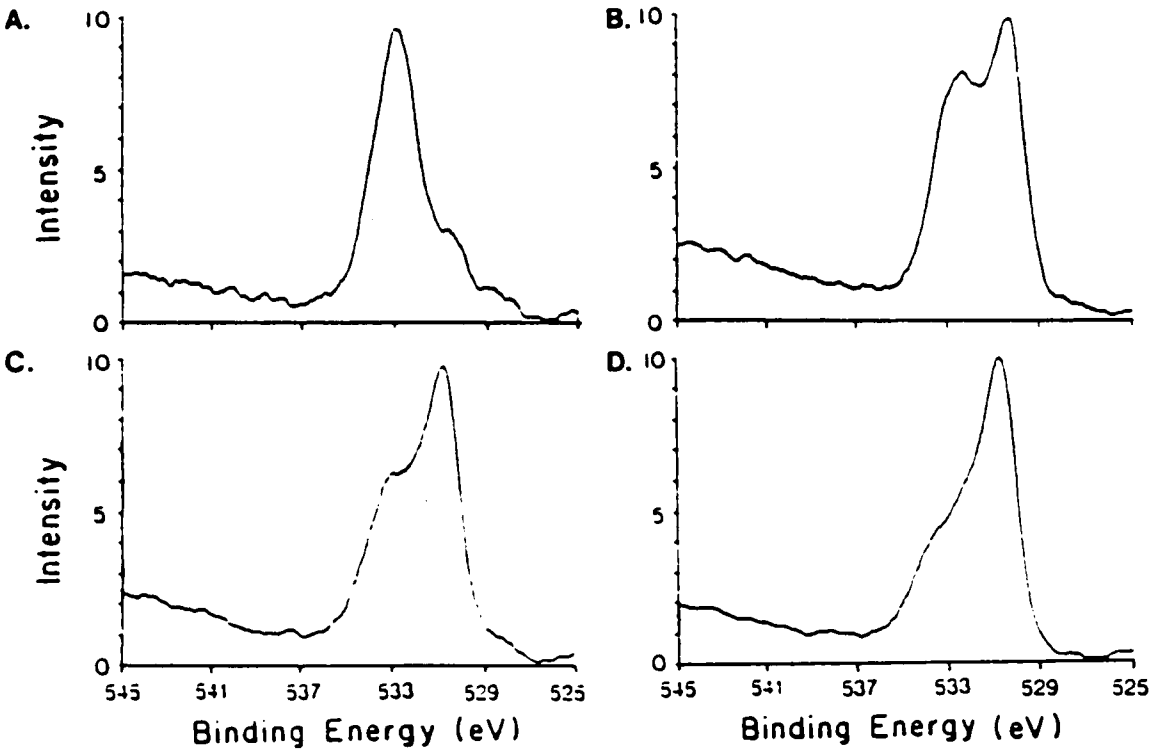

Figure A-4. XPS O1s photopeaks from Ti 6Al-4V bonded with FM-300U failure surfaces for environmentally aged samples. (A) 0 days, center section (B) 7 days, center section (C) 7 days, side section (D) 28 days, center section.

environment. Critical strain energy release rates were obtained as a function of time for environmentally exposed wedge samples and the values decreased as exposure time in hot water increased. Failure became more interfacial as the wedge samples were exposed for longer times and the diffusion of moisture was non-Fickian.

6. REFERENCES

1. F.J. Boerio and C.H. Ho, J. Adhesion, 21, 25 (1987).

2. P. Commercon and J.P. Wightman, J. Adhesion, 22, 13 (1987).

3. V.T. Kreibich and A.F. Marcontonio, J. Adhesion, 22, 153 (1987).

4. R.A. Gledhill and A.J. Kinloch, J. Adhesion, 6, 315 (1974).

5. K. Nakamura, T. Maruno and S. Sasaki, Int. J. Adhesion and Adhesives, 7, 97 (1987).

6. J.G. Mason, R. Siriwardane and J.P. Wightman, J. Adhesion, 11, 315 (1981).

7. G. Koranyi and T.M. Acs, Acta Chim. Hung., 24, 3337 (1960).

The two page vita has been removed from the scanned document. Page 1 of 2

The two page vita has been removed from the scanned document. Page 2 of 2